Performance Optimization

Of

Small Scale

Photovoltaics

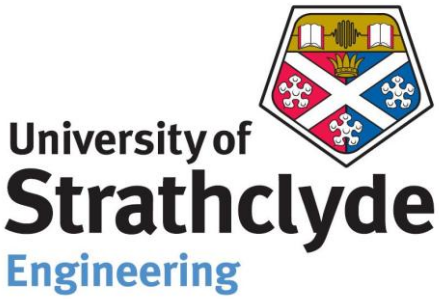

Department of Mechanical Engineering

Author: Matthew Martin

Supervisor: Mr Cameron Johnstone

A thesis submitted in partial fulfilment for the requirement of degree in

Master of Science in Renewable Energy Systems and the Environment

2010

Copyright Declaration

This thesis is the result of the author's original research. It has been composed by the author and has not been previously submitted for examination which has led to the award of a degree.

Signed: *Matthew Liam Martin* Date: 10/09/2010

Abstract

The focus of this thesis is on solar energy and specifically how to optimise the energy yields from photovoltaic panels. Consideration is given as to how this energy is generated and where losses most commonly occur. Methods of optimisation of performance and mean time between failures are investigated.

The theory behind PV generation is discussed and electrical properties and device efficiencies defined. Methods of typical power optimisation in the field of photovoltaics are investigated along with recent and current research into this area.

The specific research focuses in on the design of an experiment to test and define performance parameters for PV cells. Sensors are chosen with consideration to the further development of power optimisation and condition monitoring systems. N interface was designed with in LabVIEW and the sensors calibrated to ensure accurate results were obtained

The PV cell performance is then tested under various different conditions. Losses in performance due to various different changes are identified. Finally it's performance in considered against the use of maximum power point tracking and the impact of ignoring this as a method of power optimisation.

Acknowledgments

I would like to acknowledge the support and advice given by Cameron Johnstone throughout the project behind this Thesis. I would also like to thank him for giving me the opportunity to travel to Korea and the Maritime University to complete the research involved.

I would also like to thank Professor Oh and all the research students with in the Energy 2 Environment research lab for their kind hospitality and diligent support in developing the experiments involved in this project.

Finally I would like to thank my Family and Friends for their support in helping me throughout the course of the last year.

List of Figures

Contents

1. Introduction

One of the most contentious debates in our society today is that of global warming and its causes. The debate is generally split in 2 camps with those who believe that increased carbon emissions are the cause of melting ice caps and extreme varying weather conditions across the globe and those that feel the current trend is a natural occurrence as a result of natural changes in our eco-system. Evidence for either argument is easy to find such as the famous hockey stick graph produced by Mann (Mann et al. 1998) shown below in figure 1:

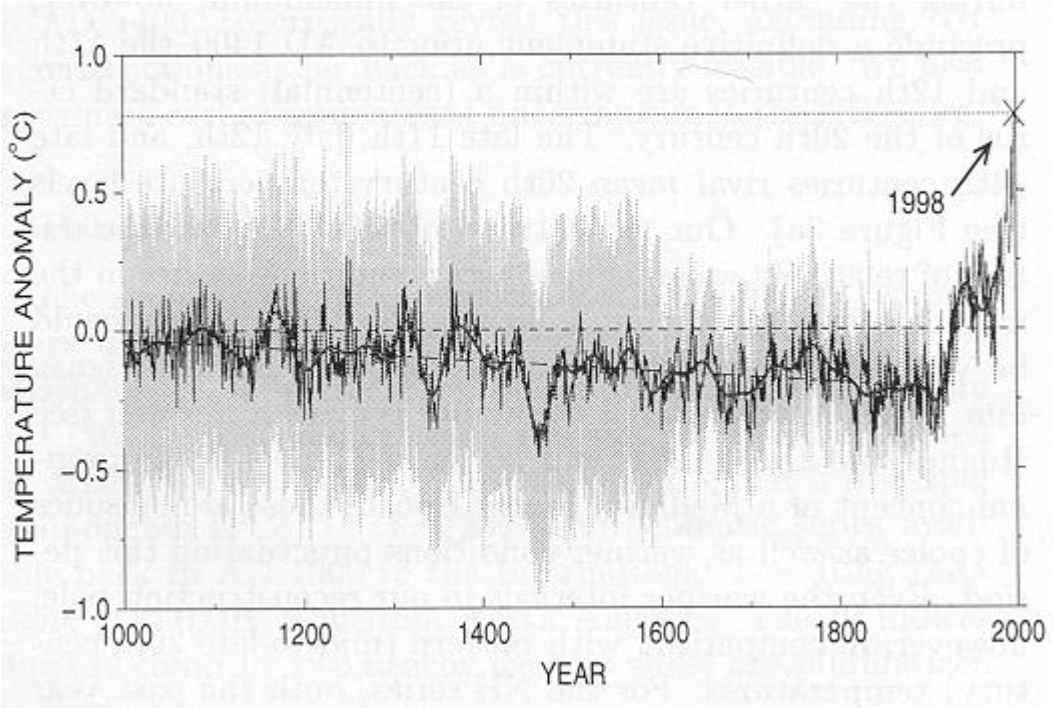

Figure 1: Global Variation in Temperature (Man et al 1998)

This graph highlights the recent trend in increasing global temperature and is an important piece of evidence used in the annually produced Intergovernmental Panel on Climate Change (IPCC) Assessment Reports which highlight current climate trends across the globe. However in recent times this has come under scrutiny with suggestions of inaccuracy in the data used (McIntyre & McKitrick 2003). This debate, coupled with disputes as to whether fossil fuel reserves are becoming depleted or not, as discussed in the IEA World Energy report 2008, is leading to questions of the need for such a push towards renewable energy resources. However the major issue of sustainability and of the resources available to

us would suggest we need to question how they are used and how we, in general, live as a western society compared with poorer developing countries.

Regardless of opinion of these issues, the British government along with the rest of the EU and many other countries around the world has agreed to a number of targets in order to reduce our national Green House Gas (GHG) emissions with a focus on CO_2 as this is seen to be one of the most significant GHG's. These agreements started with the Kyoto protocol with a long term view to tackling climate change and avoiding what is seen to be an irreversible increase of 2^oC. By 2020 the Climate Change Bill sets out a new legal framework for the UK to achieve a 26-32% reduction in Carbon dioxide (CO_2) emissions on 1990 levels through international and domestic action with aims to have reduced their emissions by 80-95% of 1990 levels by 2050. The Scottish government in fact, have set even more stringent targets upon themselves aiming to have reduced emission 42% by 2020. This decision was taken as there is a belief that, with increased resources of wind and wave resources available in the North (Figure 2,3), these targets can be easily met by Scotland. A testament to this is that as of 2006 Scotland has achieved reductions of 18% 14 years in advance of the initial target of 20% expected by 2020 **[4]**

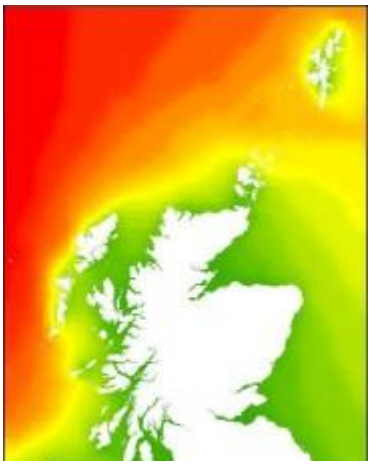

Figure 2: UK Wave resource

http://www.see.ed.ac.uk/research/IES/research/marine.html

The British government, as part of the UK Energy Act in 2004, defined micro-renewables resource as any renewable source of generation less than 50kW for electrical sources and less than 45kW for thermal generation. The following are listed as recognised renewable sources however the document does advise that any other source of energy or technology which aids in cutting emissions of greenhouse associated with the generation of electricity or the production of heat in the opinion of the Secretary of State in Great Britain could be considered as a micro-renewable resource:

- Biomass
- Bio-fuels
- Fuel Cells
- Photovoltaic's
- Water
- Wind
- Solar Power
- Geothermal
- Combined Heat and Power (CHP)

In order to achieve these reductions a number of different changes are expected to be implemented. These include a combination of a move to green fuel sources and improved efficiencies in consumption of energy through hybrid engines for transportation. Improved energy efficiency of industrial and domestic buildings including a new policy that stipulates all newly built houses are to be carbon neutral during their full life cycle by 2016. Increased sustainable or renewable energy generation including a move to a distributed energy resources with the promotion of domestic renewable generation as defined above through the Feed in tariff introduced as of April 2010 in the UK and already in place in European countries such as Spain and Germany.

In considering the built environment, both domestic and commercial, the IEA World Energy report from 2008 indicates global energy consumption increased by 37% between 1990 and 2005 with this sector consuming a 47% share of the Worlds generated electricity. This represents an increase of electricity consumption in this sector of 73% over the same 15 year period and clearly reflects the increase in use of electrical devices such as computers, televisions, indoor lighting and other modern day "convenience" devices.

This energy consumption highlights the potential for significant reduction in energy consumption in the built environment. This can be achieved in 2 ways, the 1st is demand side, both in the amount of energy used and also when it is used (demand side management). The second would be to integrate renewable energy sources alongside a grid connection and progress to a stage where demand side management would reduce grid consumption to a bare minimum and maximise use of any renewable energy generated by available resources such as wind or solar energy. In this instance micro-renewable generators would be installed on the building it-self to provide alternative energy resources.

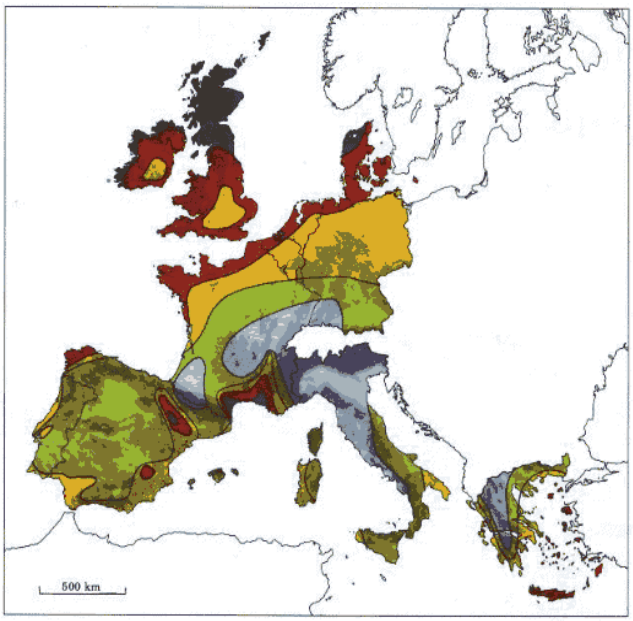

Figure 3: European Wind Resource

http://www.esru.strath.ac.uk/EandE/Web_sites/03-04/wind/content/eu_windmap.html

2. Solar Energy

2.1 Source

One of the most common and well known sustainable energy resources in consideration of a future energy supply is that of solar energy. Solar energy is that which is radiated from the sun and incident upon the earth. It heats the air around us and provides energy for plants and is even the source of shallow surface geothermal energy. The energy travels in the form of electromagnetic waves across a large range of wavelengths with waves between 250nm and around 2500nm (Figure 4) wavelengths reaching the Earth's surface (Möller 1993). In fact the amount of energy as a result of this radiation incident on the Earth's surface annually is between 800kW/m^2 and 2200kW/m^2.

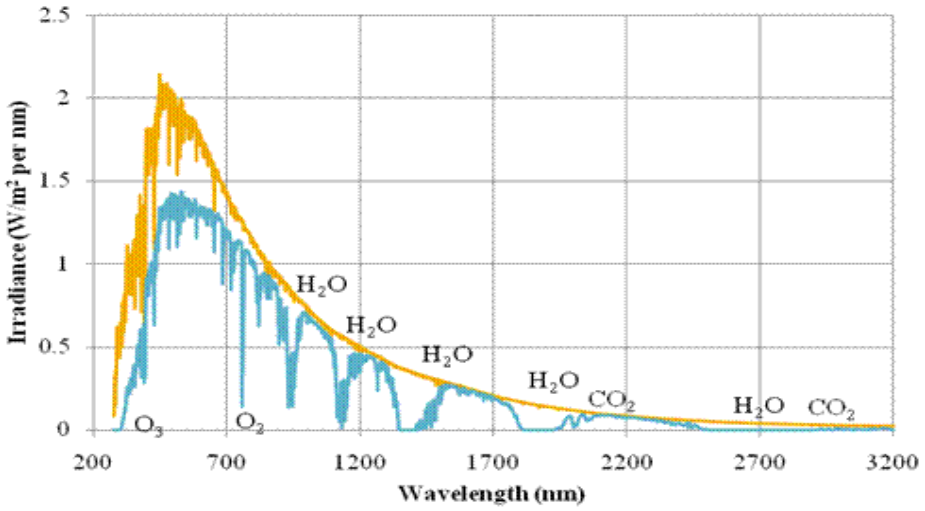

Figure 4: Solar Radiation Intensity
http://homepages.ius.edu/kforinas/ClassRefs/GlobalWarming_files/greenhouseeffect.htm

This energy is generated at the core of the sun in a nuclear fusion reaction where temperatures reach 10^7K, hot enough for hydrogen atoms to be fused together. The energy from this reaction is emitted as x-rays, gamma rays and high energy neutrinos and this energy in turn heat up the outer gasses of the sun to around 5800K. It is these outer layers that then radiate energy to Earth and the surrounding planets. Of all the radiation that does reach the Earth, around 30% is attenuated before reaching its surface.

Considering even these conservative estimates of 800kW per square meter and assuming the Earth's surface area to be roughly $5.1x10^8km^2$ that would mean there is roughly $4x10^8$TW of energy available to be converted to useful energy. Even if we only consider the surface area that is land mass this still comes out at around $1.2x10^8$TW. Clearly there is an abundance of this energy that if exploited correctly could remove any need to rely on fossil fuels.

2.1 Methods of Conversion

There are a number of methods of utilising such energy and can be defend as passive or active. Passive methods generally involve the manipulation of this solar radiation for heating and cooling purposes. Typically this can involve the design of a building to maximise or minimise the amount of solar radiation entering an occupied space. For example even in considering the orientation of a building can be considered to be a passive design technique as a southward facing window in the northern hemisphere will see increased direct solar radiation and thus experience increased heating during the day. Seasonal variations can also be exploited with the use of a sun awning. During the summer months when the sun is high in the sky the awning reflects any direct incident solar radiation so as to reduce natural heating of the occupied space and thus reduce any cooling loads that may be required. In the winter months the sun is lower in the sky thus allowing the same direct solar radiation too enter the same space increasing natural heating and reducing any extra heating that may be required.

More complex design techniques include Trombe or solar walls. These are south facing walls consisting of 3 layers; a glazed external layer, a small air gap and an internal concrete wall. The glass allows solar radiation to pass through and heat up the trapped air, it also minimises the amount of solar radiation transmitted back out of the air gap to maximise this heating effect. The heat is then conducted through the concrete wall throughout the course of the day, reaching the internal surface in the evening when heating is required as the sun sets and the ambient temperature drops.

As well as space heating solar energy can be used for hot water. A solar thermal heater uses an antifreeze solution to absorb infra-red solar radiation; this heated solution is then passed through a heat exchange to heat up a small hot water supply thus reducing the demand on a gas or electric boiler.

Active methods of exploitation of this energy include solar thermal power plants. This is where the heat absorbed form solar radiation is used to power a large steam turbine to convert this energy to electricity. This is done in the same way as a standard steam turbine where the solar energy is absorbed using a gas with a low evaporation point and this is used to drive the turbine as it rises up.

All of these methods involve the conversion of solar energy to heat however there it can also be converted to electricity through the photo-electric effect. This method uses a semi-conductor material to convert electromagnetic radiation into a direct electrical current normally made of silicon doped with a small amount of another material such as Phosphorus, Arsenic, Boron or Aluminium (Neamen 2003) to increase its ability to convert light to electricity. Other materials such as Copper Indium Diselenide and Cadmium Telluride have also been used (Birkmire & Eser 1997). Performance of these materials can vary but is typically anywhere from 6 to 17%. This low efficiency may seem off putting for such a technology in comparison to traditional fossil fuel plants with efficiencies of round 40% and nuclear power with efficiencies of 80%. However if we consider a low 6% conversion efficiency of the minimum amount of annual solar radiation this still results in a conversion of 7.2×10^{6}TW of energy.

2.2 Photo-electric effect Theory

In order to understand how photovoltaic cells operate we must understand a number of scientific principles the 1st of which is the photo-electric effect. The 1st observation of the photo-electric effect was by French scientist A.E. Becquerel in 1839 (Markvart 2003). While experimenting with electrolytes he noticed a chemical reaction occurring as a result of exposing a silver halide rode immersed in an ionic solution to light, this 1st observation was of a photo-electrochemical cell conducting electricity through ions. Einstein later went on to define this as the photo-electric effect in 1905. He described how the energy in an electromagnetic wave can be considered to be contained in discreet bundles and called these discreet packets photons. He went on to suggest that these photons could be absorbed by an atom and, if they have sufficient, energy result in the release of an electron free to conduct electricity thus producing the effects witnessed by Becquerel.

While semi-conductors were in use before the development of this quantum theory, it was only with these ideas and the work of scientist such as Schrodinger, Pauli and Heisenberg, to name but a few, that the advances in semiconductors required to design a PV panel came about. This idea of electron excitation eventually led to the development of the p-n junction, the foundation on which a photovoltaic cell is built.

In order for electricity to be efficiently conducted through a semiconductor it 1st needs to be doped. This is the process of adding a small amount of impurity to the semiconductor crystal so as to promote the number of current carries within the crystal. Depending on the type of doping material added this can result, in the case of a p-type material, an increase positively charged holes (gapes where electrons would normally appear) or in the case of n-type material an increase in excess negatively charged electrons. These materials can then be combined to produce a p-n junction across which a current can flow through these excess carries (Figure 5)

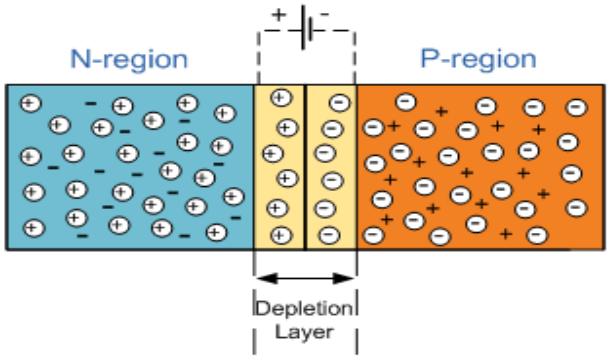

Figure 5: pn junction
http://www.electronics-tutorials.ws/diode/diode4.gif

In order for this current to flow the circuit must be connected in forward bias so as to move the majority carriers (electrons and holes) away from their relevant terminals. The coulomb or electrostatic force in the circuit drives holes in the p type material away from the positive terminal towards the junction with the n type material and vice versa the negative terminal drives the electrons towards the p type material. It is thus common to have a thin layer of heavily doped n type material above a lightly doped p type material in the construction of a PV cell as in Figure 6 below.

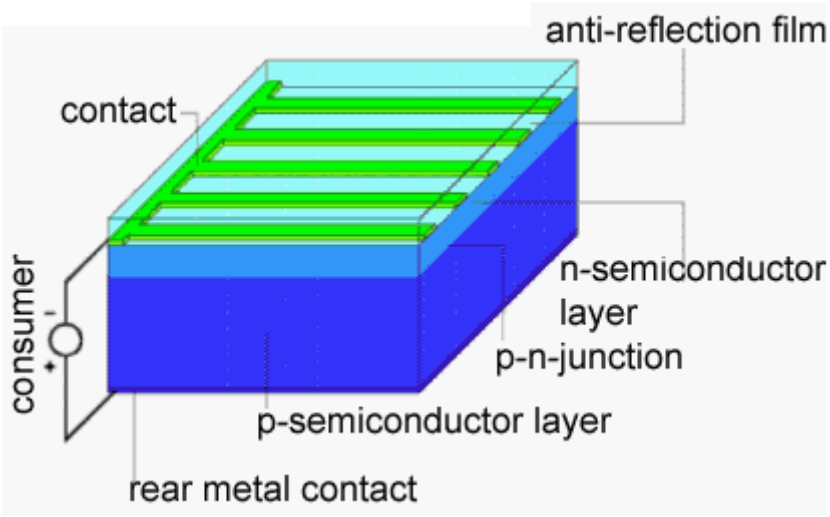

Figure 6: Solar Cell

http://www.solarenergyireland.com/Information/solar_electricity_and_solar_cells.html

In considering the construction of a single PV cell there are 3 different crystal structures that can be doped to provide the required efficiency for a photovoltaic cell, these are poly-crystalline mono-crystalline and amorphous. Each type dictates cost and performance:

Mono-crystalline – This is made of a single crystal of atoms such as silicone. Processes used to grow such a crystal include the Czochralski or float-zone process (Möller 1993). In the case of Gallium Arsenide Single crystal structures were more popular in the beginnings of PV design as while these processes of construction were expensive they produced relatively efficient cells in comparison to polycrystalline structures. The increased expense is due to the limitations in the size that these crystals can be grown to, usually around 10 cm in diameter. This obviously means a larger number of crystals cells would be required for a single panel to be built thus increasing costs.

Polycrystalline – These crystal structures are far less efficient that their mono-crystalline counterparts and have only more recently come into commercial use as efficiencies have been improved while keeping growth costs to a minimum. The 2 most common growth processes are ingot and ribbon or sheet growth (Möller 1993)*).* Ingot growth produces cells on a comparable size with typical mono-crystalline cells produced in the Czochralski process at a reduction of only around 30% of the cost. The ribbon method looks to produce thin films directly. This removes the need for the thin slicing required of large crystals which usually results in a loss of 40-50% of the material grown. This reduction in waste material and the removal of the slicing process results in reduction in the overall cost making their use more preferable to mono-crystalline. Improved efficiencies in polycrystalline cells coupled with the reduced manufacturing costs mean more modern designs have turned to these cheaper designs.

Amorphous - These compounds have the advantage of being processed at a significantly lower temperature than mono or polycrystalline ones which require temperatures above 580^{o}C. Instead these amorphous materials can be processed at temperatures of 250 – 300^{o}C. Electrical conductivity is promoted through the use of PH_3 or B_2H_6 which release hydrogen that binds to the silicon structure during decomposition.

These resulting crystals grown from the above processes are primarily used in the construction of micro-processors. The excess or waste from the cutting stage is then re-processed for use in the construction of PV cells. This means in 2000 when approximately 18,200t of silicone was produced for the electronics industry, after processing of post process silicon, around 13% was left for PV production or 2,366t(Woditsch & Koch 2002). Woditsch and Koch predicted that by 2010, if the PV sector grew as forecasted, we would require in the region of 8,000 – 12,000t. In fact by 2003 the predicted growth had risen to 32,000t required for the pv industry alone. This figure indicates the significant growth in the uptake of PV as tougher climate change targets are brought in to place and with growth beyond commercial use to domestic and business implementing small scale PV arrays for cheaper electricity.

3. PV Power Generation

3.1 Electrical Properties

In order to maximise power from a PV panel we must a number of electrical properties of the photovoltaic cell, these include the open circuit voltage V_{oc} and the short circuit current I_{sc}. The open circuit voltage V_{oc} (where there is a potential difference but no current) in this case refers to how strongly the photo-generated charge can bias the pn junction under a given level of illumination. It is determined by the ratio of photo-generated current I_L (the maximum current that can be generated in a pv cell) and the saturation current I_s as can be seen in equation 1 which is derived from the ideal pn-junction current-voltage characteristic equation (2). This means that it is based around the cells efficiency and ability to absorb photons:

$$V_{oc} = {}^{KT}/_{e}\, ln\left\{\frac{I_L}{I_S} + 1\right\} \quad (1)$$

$$I = I_S\left\{exp\, {}^{eU}/_{KT} - 1\right\} - I_L \quad (2)$$

The short circuit current, $I_{sc,}$ is that which causes current through the load to be less than the photo-generated current it is determined by the cells quantum efficiency in converting incident photons into electron-hole pairs at any given wavelength. It is equivalent to the photo-generated current I_l when the series resistance in the panel is equal to 0.

These values can be obtained by plotting a current-voltage curve graph. This done by varying a small resistive load from zero to several kilo-ohms while the cell is illuminated and measuring the voltage and current outputs the current is then plotted as a function of voltage. The resultant graph takes the form as seen in Figure 7 over the page:

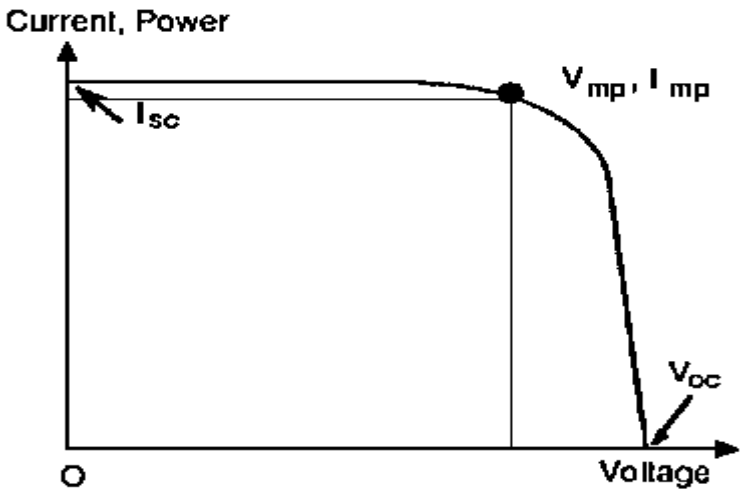

Figure 7: PV I-V Characteristic Curve

http://engnet.anu.edu.au/DEpeople/Andres.Cuevas/Sun/help/PVguide.html

At the point where voltage and current are at their maximum, highlighted above as V_{mp} and $I_{mp,}$ the power output from the PV panel is at its maximum. In general a solar cell will be operated at this maximum power point. This is normally done by varying the load on a cell so that it operates at as close a value to this point as possible. The efficiency of a PV cell can then be easily related to these values:

$$\eta = \frac{P_{out}}{P_{in}} \quad (3)$$

Where $P_{out:}$

$$P_{out} = V_{max} I_{max} \quad (4)$$

Substituting eq3 into eq4 we find:

$$\eta = \frac{V_{max} I_{max}}{P_{in}} \quad (5)$$

3.2. Efficiencies

It is important to understand the overall efficiency of a solar cell as this plays a significant part in the overall output power of the cell. The efficiency of the solar cell can be related to I_{sc} and V_{sc} by considering the fill factor (FF). The fill factor refers to a measure of the actual possible power that can be generated from a PV cell, (the area contained within the square in Figure 7, previous page) it is quantified by the ratio of maximum voltage and current to Short circuit current and open circuit voltage:

$$FF = \frac{V_{max} I_{max}}{V_{oc} I_{sc}} \quad (6)$$

Rearranging eq 6 and substituting it into eq 5 we then see there is a direct relationship between the PV cell efficiency and the open circuit voltage and short circuit current:

$$\eta = \frac{FF\, V_{oc}\, I_{sc}}{P_{in}} \quad (7)$$

This then indicates that if we maximise V_{oc} or I_{sc} we can increase the overall efficiency of the PV cell. There are however some limitations to this in practice. The open circuit voltage is limited to the built in voltage, if it exceeded this level then the built in field of the pn junction would be cancelled out limiting the minority carriers to the quasi neutral regions. As it is also linked to the saturation current (eq 1) and limited by how small a value of this can be achieved. This is intrinsic to the material used as it is determined by the recombination of carriers within the semiconductor material which is dependent on the size of the energy band gap that an excited electron must cross. An increase in the band gap results in decreased saturation current. The short circuit current is related to the photo-generated current with this being the maximum allowed value. This is also related to the band gap energy, with smaller band gaps allowing for more photons to generate electron-hole pairs and thus generate a maximum current. This conflict indicates there is a point where

increasing the size of either property will result in a reduction of the other and so there is a point where each value is optimised so as to achieve the maximum possible power form the pv cell.

Temperature also plays an important art in the overall efficiency. Over a wide temperature range there is a slight improvement in the short circuit current. This comes from increased thermal velocity of minority carriers with in the p doped material. This increased thermal velocity means these carriers are less likely to recombine with majority carriers and so they are more likely to reach the junction and on to the transmitter. This means as the temperature is increased so too is the photo-generated current and as the short circuit current is directly linked to this, as mentioned above, there will be a slight increase in this value too.

When considering open circuit voltage however there is a marked decrease in this value with increasing temperature. This due to its dependence on the saturation current, which is it-self in turn dependent on the intrinsic carrier concentration of the semiconductor. As temperature increases so too does the carrier concentration and thus the saturation current so as explained above, with increasing saturation current there comes a decrease in the open circuit voltage. When taking the logarithmic nature of this relationship the decrease in V_{oc} with increased temperature is almost linear.

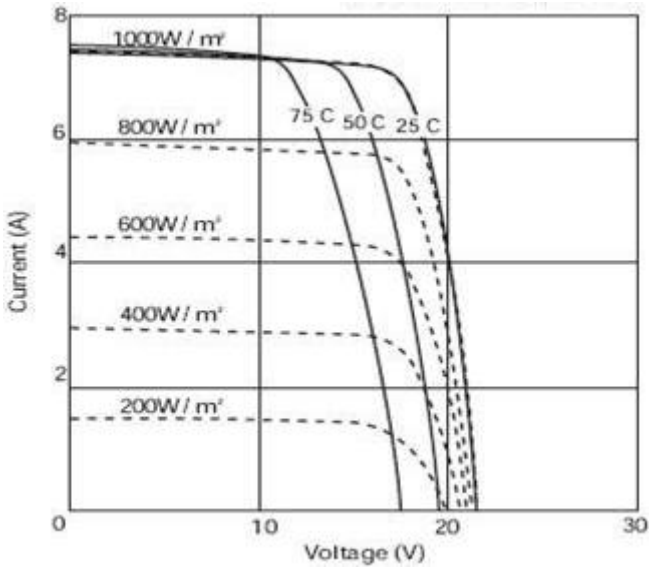

Figure 8: I-V Thermal Variation

http://www.altestore.com/howto/Electrical-Characteristics-of-Solar-Panels-PV-Modu/a87/

The ideal pn junction would have a square like I-V graph thus allowing for the optimum power conversion however, as can be seen in Figures 7 and 8. the graph is slightly rounded. The areas outside the fill factor square indicate losses due to shunt and series resistance. Shunt resistance is that which occurs due to high conductivity paths within the cell structure or around the edges. Causes of these paths include lattice defects within the depletion zone of the pn junction and leakage currents around the edges of the cell. These can arise as a result of structural defects of the semiconductor crystal such as dislocations, grain boundaries and large precipitates. Series resistance is a combination of the bulk resistance of the semiconductor and the resistance of contacts at the surface of the semi-conductor and at the metallurgic contact of the pn junction.

In order for the I-V curve to take on this ideal square shape zero series resistance and infinite shunt resistance would need to be achieved, however this is clearly not feasible. Instead it is preferred to maximise shunt resistance while minimising series resistance. Low shunt resistance will result in a degradation in the cells output voltage $V_{out,}$ while a high series resistance will see a drop off in the output current I_{out}. Shunt resistance can be as low as 100Ω (Möller 1993) before there is any noticeable drop in performance however it is more common that shunt resistance is in the region of 500Ω (Mazer 1996). While this clearly shows the scale in which shunt resistance can vary, the output power is much more sensitive to series resistance. *Möller* in fact suggests that a series resistance of as much as 5Ω can result in a drop in performance of as much as 30%. Therefore it is common to find series resistance is kept to as low as between 0.5-0.7Ω to ensure these losses do not occur.

So it is clear that there are a number of factors that affect the efficiency and performance of a PV cell, from the design of a single cell it-self right down to the atomic structure of the semi-conductor crystals used in the construction of the pn junctions. As much as these areas have been investigated and researched over the last few decades to find areas for improvement of performance (Jahanshah et al. 2009)*),*(Kostic et al. 2010) very little in the overall efficiencies has been made. Even with cell efficiency maximised the upper theoretical limit of conversion is around 40% with a cell temperature of 300K. This is based on the treatment of both cell and sun as blackbodies, those which are perfect emitters and absorbers of solar radiation. If thermodynamic principles are taken into consideration this drops to between 30 and 37%. In the early 80's efficiencies were in the region of only 8% (Braga et al. 2008) in the commercially preferred polycrystalline cells with only marginal increases to between 10 and 13% by 1990 (a 2-5% increase over 10 year period) and only achieving

15% experimentally by 1996. In fact presently this level of conversion is the norm for polycrystalline cells, with more costly mono-crystalline cells only achieving marginally higher conversion efficiencies of around to around 2

It is clear then that while there is limited room for minor improvements in solar cell conversion efficiencies, these will be very limited. It is then vital that any power generated is itself used as efficiently as possible. This is being done in a number of ways including use of condition monitoring and power optimisation.

3.3. Condition Monitoring

Condition Monitoring is the practice of implementing various to optimise mean time between failures of equipment while increasing long term operability of these machines. It is common practice in all areas of engineering including the oil and gas industry, civil engineering, aeronautics and is now finding a place in the renewables sector. It is most commonly used in the measurement of mechanical properties such as stresses and strains in structures as well as vibration and acoustic monitoring however process such as Thermography (de Brito Filho & Henriquez 2010) are finding use in the electronics industry. Her they can be used for the monitoring of hotspots in circuits where potential faults may be developing that could potentially lead to failure in the board or a component of the circuit. While there have been examples of the use of Thermography in experimental measurements of PV properties (Konovalov et al. 1997), there is no reason this could not be expanded upon to be used in a similar way as in the electronics industry to help identify faults with individual cells in a panel and either allow them to be bypassed or repaired to ensure continued optimal performance in the whole panel.

It is also common place to monitor the electrical properties of a system such as a generator. Methods such as Motor Current Signature Analysis (MSCA) can be used to identify vibrations within a gearbox through fluctuations of the frequency of the generated current (Kar & Mohanty 2006). In the same way variations in current and voltage could be measured and any variations used to identify faults through predefined analysis. Frequency analysis would not be so simple, as the power generated by the pv cell is dc and so needs to be converted by a dc-ac inverter. This means considerations of the effect of the inverter on the output frequency would also need to be taken into considerations in any algorithm or model to be used in this process.

It is important to understand though that condition monitoring is aimed at increasing the operating life time of a device and increasing the mean time between failures. So while this will help to maximise the overall power output of a generating device over its life time it does not increase the instantaneous use of any available power. This requires a different approach on a more small scale temporal level.

3.4 Power Optimisation

Power optimisation is required to ensure what power generated by the PV cell is being used efficiently. This is important as the conversion efficiencies as discussed previously are so low and so as a move away from fossil fuels is made it is vital that the maximum amount of generated energy possible is used. In order to both maximise and get the best form the power generated from a PV cell a number of different methods can be applied.

3.4.1 Tandem Junctions

At a structural level tandem or multilayer junctions can be implemented to absorb as much solar radiation as possible. The idea is to us materials with slightly increasing or decreasing band gaps. There are 2 possible methods of construction. On uses mirrors to direct light of varying wavelengths on to the surface of the semiconductor with the appropriate band gap for that wavelength of light to be absorbed. A more common method that fits with modern thin film pv panels is to use a number of layers stacked on top of each other to absorb different wavelengths.

The 1st layer will absorb photons of a specific frequency of energy equivalent to that of its band gap, this material is effectively invisible to any photons below this level as their energies are too low to excite an electron and create an electron hole pair. Any photon with an excess of energy above that of the band gap will result in electron-hole pairs that simply recombine. This means a number of photons will effectively pass straight through to the next layer. Here a material with slightly larger or smaller band gap will absorb any transmitted photons with higher or lower frequency than the previous layer and so on layer by layer as is shown in image 8 over the page:

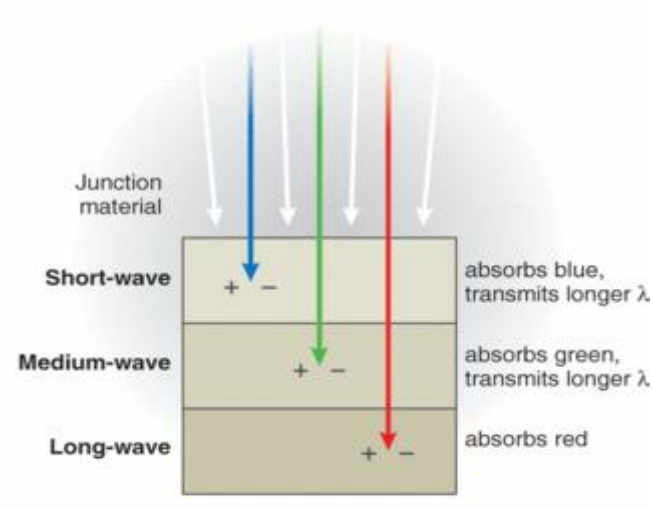

Figure 9: Tandem pn junction

Typically the multilayer structure is designed with the 1st layer absorbing the high energy electrons, those with a shorter wave length i.e. those at the blue end of the spectrum of visible light. The next layer absorbs those photons with lower energy in the middle spectrum with the 3rd and final layer absorbing low energy photons at the red end of the spectrum. Each layer is separated by a heavily doped substrate to allow carries to quantum mechanically tunnel from one layer to the next. Typically the sorts of structures take the above 3 layer approach as any more than 2 tandem junctions is difficult to manufacture although. This method allows for the maximum amount of solar energy to be absorbed.

This method is still more related to efficiency of a single PV cell. In order to optimise performance of the PV panel a process such a solar tracking can be used to ensure solar panels follow the optimal position of the sun in the sky based on their geographic location and the time of year (seasonal variances result in varying height of the sun in relation to the horizon). Methods used to track the sun include passive systems that use a liquid that will expand and contract depending on the amount of solar radiation incident on. This can be exploited in a hydraulic system so as to ensure the panels are at the optimum angle to absorb incident solar radiation. This setup is comparatively cheap but not completely accurate. A more accurate method of solar tracking active uses a number of small photodiode sensors to measure instantaneous light intensity at different points and uses this collated information to adjust the system as required.

More recently this has been superseded by development of microprocessors. This means accurate solar and climate data can be stored and used to adjust the panels as required for optimal performance. Use of IT systems, while more accurate, is much more costly and so tends to be more suited to large installations of PV panels such as solar farms.

3.4.2 Inverters

Between the PV panel and load it is supplying usually lies the dc-ac inverter. At this point of connection there are a number of considerations to be made to ensure optimal performance. The inverter efficiency dictates the required PV power for a given AC output and therefore the number of PV panels required for operation of a system. It controls the shape of the magnitude of the output voltage of the ac converted current from the PV panel. The shape of the output wave will determine the type of equipment that can be connected.

In this case there are 3 different types of wave out-put: Sine wave; modified sine wave and square sine wave (Norton et al. n.d.) . The sine shaped ac output will allow operate with the majority of commercial equipment as too will a modified sine wave output which produces a square like supply with an extra step up or down. Square wave output inverters will generally only work with simple equipment like a universal motor but they are much cheaper and can be modified to produce sine waves with a power filter however this does add another point of failure to the system.

The overall inverter efficiency is also dependent on the proportion of its maximum rated power that it operates, the closer to this value the more efficient the device works. This can depend largely on load size and inverter configuration. In terms of the overall load for an input power between 30% and 50% of the inverters rated power an efficiency of 90% can be achieved (Norton et al. n.d.).

Standard configurations of inverts can include Sole inverter, multiple string inverter, integrated inverter and master slave inverter. A sole inverter is usually supplied by several PV panels connected in series. A DC bus switches these in parallel. This means a complex DC setup is required however costs are kept low and efficiency is generally very high.

Multiple string inverters rely on several panels connected to a number of inverters so that each inverter can operate at or as near as possible to its peak capacity. A master-slave configuration also entails multiple cells with multiple inverters connected together. However in this case at low levels of solar radiation the whole string is connected to just a single inverter operating the inverter at its peak input power level, when solar radiation levels increases the PV array is divided progressively into smaller units, until every string inverter operates independently at or near its peak rated capacity. Each of these configurations involves increased cost but does however provide increased redundancy over a single inverter set up. Master slave configuration also provides continually high efficiencies however it is the more costly of the 2 configurations.

Module-integrated inverters are typically located to the rear of each PV module, converting that panel's DC output directly. This provides a number of advantages but also several disadvantages. The disadvantages include increased heating of the module due to the inverter being directly connected to the panel. This will result in increasing the number of thermal recombination's in the semiconductor reducing it' overall output. The zero load dissipation is increased in comparison with other set ups and the overall cost means it would likely be cheaper to use a centralised inverter system such as those mentioned above. The benefits however include reduced losses due to less cabling between source and inverter. This also has the added benefit of reducing cost due to less cabling and fewer losses through transmission of high voltage low current ac power. Transmission also has the added benefit of improved safety through reduction of any high DC voltage transmission that would otherwise be involved with other configurations. Finally Maximum power point tracking is local to each cell and so losses due to mismatching of power out and the converter rated power can be kept to a minimum.

3.4.3 Maximum Power Point Tracking

An important part of the inverter and the overall output power of any array of PV panels is the maximum power point tracking (MPPT) system. It's is typically installed within the inverter unit itself and uses power electronics to ensure power out from the inverter is maximised. It is based on the idea of the maximum power point and its relation to V_{max}, I_{max} and FF of the I-V curve of a PV panel. It uses advanced algorithms to track the maximum power point of a PV cell based on variations in temperature and solar radiation so as to ensure the maximum power is supplied at any given time.

The power out is controlled by varying the input voltage drawn from the PV panel, ensuring it matches, or is as close as possible to, the expected V_{max} at any given point in time. There has been a lot of research in to various different algorithms for this type of control as, while it is costly it ensures PV arrays operate at their optimum levels. These algorithms include the constant voltage method, perturbation and observation (P&O) method and incremental conductance (InCond) method. Recent research has looked into considering how these algorithms could possibly be combined (Yu et al. 2004) so as to further ensure accuracy in tracking of the V_{max} value and therefore the maximum power output for the PV/Inverter system.

The constant voltage method uses a numerical analysis method to find a linearly approximate relationship between the current of MPP and the photocurrent which is directly proportional to the solar radiation incident on the panel. This method is best suited to areas where there is little variation in the ambient temperature as this any large temperature variations can influence carrier recombination therefore affecting the photocurrent without being incorporated into the computation.

The P&O method moves the operating power point towards the MPP by periodically increasing or decreasing the converter input voltage and adjusting. While it is commonly used in PV arrays it does have problems in that it fails to track any sudden or rapid change in solar luminance and hence incident solar radiation on the PV panel thus missing any sudden increase or decrease in output voltage.

The InCond method is the more complex of these 3 methods and requires 4 sensors to make measurements of the solar panel conductance and compares incremental values with instantaneous ones. While this method is very accurate it does however have a temporal issue whereby any excessive processing time that might be required by sensor or system can result in the loss of a large amount of power.

3.4.4 Current Research

Recent research has also looked into the possibility of using current as the trigger value for MPP (Jain & Agarwal 2007). This it is suggested that this algorithm will prevent instabilities associated with reference current tracking by preventing the system to move toward then positive slope of the I-V curve. The research also suggests that the algorithm is able to respond quickly to environmental changes which would prove advantageous over the continuous voltage method which struggles with any temperature variance and P&O method which fails to respond quickly enough to rapid changes.

Other research looks to improve upon P&O tracking by using simple computations and a single voltage sensor to measure and continuously track the maximum power point (MPP) (Dasgupta et al. 2008). This also claims to avoid issues with response during atmospheric changes. The research also proposed a method of self-tuning so as to considerably improve dynamics and steady-state performance.

It is clear to see that MPP is of significant importance in the utilising the optimum power generated by any number of PV panels. However the cost involved with power electronics and developing such algorithms mean that the costs of implementation can be comparable to that of small scale PV installations. It may then be worth considering alternative options in the domestic, built and rural environments where cost of installation and maintenance would be preferably kept to a minimum.

Alternatively it may be worth considering a directly coupled method where by the I-V load characteristics are as closely as possibly matched to those of the PV panel it is coupled too. The problems in this instance are if a panel is over sized then energy is wasted. Although this is not so much an issue with the introduction feed in tariffs in the UK since April 2010, it

stills means increased initial outlay. However if the panel is under sized any drift from maximum power may result in failure of equipment to operate as and when required. An example of research into improving optimisation of directly coupled PV panels is that into PV powered water pumps (Firatoglu & Yesilata 2004). This research indicates that with carefully collated date it is possible to accurately select the optimum PV array size. Data required includes long term hourly meteorological for site location, optimal PV slope, solar radiation availability and utilization, and electrical configuration details based on statistical parameters. This research indicates if performed correctly that sizing accurately will allow for performance close to MPP over a single day and over the course of a year.

Other methods of optimising energy yields from PV panels include combination with solar thermal water heaters. This gives the benefit of cooling the panel to improve generation efficiency through reduction in thermal recombination and also increases the use of infrared solar radiation in heating the water which might otherwise not be absorbed by the PV panel. This is highlighted in the following research (Fraisse et al. 2007), (Dubey & Tiwari 2008).

So clearly there are a number of different methods to extract the maximum possible energy yields form photovoltaic cells and no doubt there will be further innovations to further improve their performance. The considerations of the experiment that follows are to consider the benefits of MPPT against their cost of implementation in comparison to the overall cost of installing small scale photovoltaic cells in both the built environment and more isolated locations.

4. Joint Research Projects

In considering how performance optimisation might best be implemented, with respect to maximising varying resources renewable resources to aid in the reduction of energy consumption in both remote locations and the built environment, the Korean Maritime University (KMU) proposed and developed 2 very different research projects. Each looked to exploit a combination of a number of different renewable energy resources and the research was completed in conjunction with the University of Strathclyde.

4.1 Navigation Buoys:

The 1st project is the development of a number of navigation/weather buoys (Figure 10), each with a combination of 2 or 3 different micro-renewable resources onboard to power instrumentation. These alternative resources are being considered as an improvement on an existing system which relies on a combination of PV panels and batteries. This system uses a simple charge and discharge process to power on board equipment. Issues with this current method of powering such a system include variability in light due to seasonal variations and as a result of poor weather conditions. Also irregular charging and discharging of the battery store will reduce its operating life time resulting in increased maintenance which is not ideal for such a remote system.

Figure 10: Navigation Buoys

In considering potential renewable resources it was clear that only 3 types could be efficiently implemented in such an environment. These were identified as being solar (already in place), hydro (wave generation) and wind. As such a number of different buoys were designed with various combinations of each resource (see Figure 11). The PV systems used were 60 Watt poly-crystalline panels, WEC turbines, of a 3 and 4 bladed aerodynamic drag type, and Wells and Impulse generators were used for the wave generation. It was expected that, through a combination of these different renewables and implementing a suitable control system, the operating life time and thus overall power output would be maximised thus reducing any need for unscheduled maintenance and improving overall operating costs of such a design.

	Solar	Wave (wells)	Wave (impulse)	Wind (4 blade)	Wind (3 blade)
A	x	x			
B	x	x			
C	x	x			
D	x		xx	x	
E	x	x	x		x
F	x	x			x
G	x		xx		

Figure 11: Installed renewable generators

It was also suggested that there may be scope for these buoys to provide short term forecasted weather information to better enable coastal cities and towns to manage heating and electrical demands through early identification of incoming weather conditions. This would be transmitted back to shore along with operational data through a wireless system yet to be confirmed.

4.2 Sustainable Container Unit:

The second project looked into the development of a small sustainable container unit (Figure 12). This Unit looked to use an optimised combination of wind and PV generation alongside a standard grid connection with minimal draw. The research work done by the Energy 2 Environment group (E2E) at KMU focused on a control system to achieve this optimisation of any power generated by the renewable resources in order minimise any power drawn from the grid. The research looked at the effectiveness that pulsed width modulation could have be to limit the amount of grid drawn power based on load demands and real time generation data from the sustainable resources. In order to test this design a small fan and air-conditioning unit were installed and the system's ability to maintain a constant temperature assessed.

Figure 12: Sustainable Container Unit

Figure 13 below shows the proposed layout of the components for the circuit connecting the PV panel to the required loads. As can be seen from this diagram the nature of the experimental set

up did not allow for a wind turbine to be directly connected to the container. Instead the decision was taken to use data collected from the container unit PV panels and combine this with data received from a previously installed wind turbine on the roof of the KMU building. This would allow for predicted grid requirements to be estimated without the purchase of a new turbine or relocation of the original one.

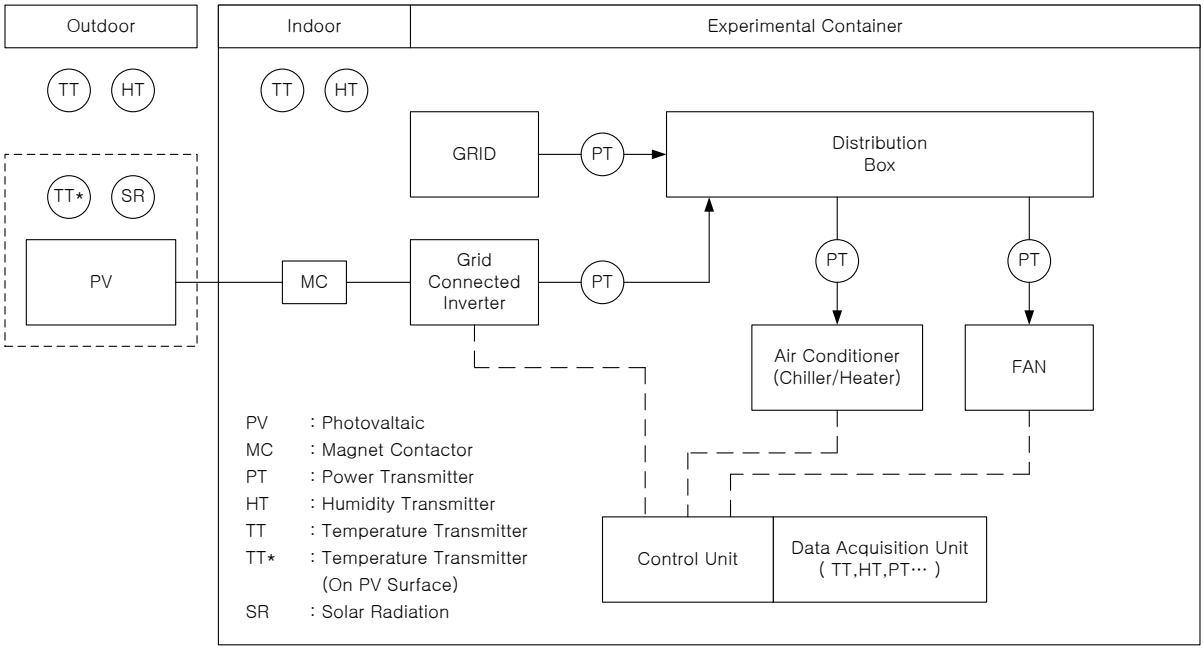

Figure 13: Proposed PV installation

With the scale of both of these projects being relatively small in their capacities it was intended where possible to keep costs to an absolute minimum. As such consideration were made as to whether there was any benefit to be had in directly coupling the container loads to the PV units and thus avoid the use of MPPT within the inverter unit. It was thought that this might also prove useful in the navigation buoys where there was potentially no need for an inverter to be installed at all. The benefit here was the removal of a point of failure in the system thus increasing the system robustness and reducing maintenance costs over the life time of the system. There was also the added benefit of reduction in initial capital costs.

Due to the remote location of the navigation buoys it was felt that some sort of condition monitoring system might be advantageous so as to further ensure minimal maintenance was required. This would further enhance annual yields through increased operational time. There was also scope for this same system to be implemented within the sustainable container unit as it would also greatly benefit from improved generation efficiencies through CM as this would reduce any down time of the sustainable generators of the system. If implemented such as system would further aid in the decision to operate such a system without MPPT.

4.3 Proposed Condition Monitoring System

The idea was to create a small Java application using a 3 gateway system to identify and alert users of any faults within the system as shown in Figure 14 over the page taken form a proposed research paper. It was suggested that the following checks might be made: the 1st stage would identify any potential faults on any of the renewable generators based on known operational data of that device; the 2nd stage would compare generating performance against climate data to identify any anomalies that may account for performance issues; the 3rd stage would check performance data in comparison to the performance of other devices operating in the same area. After completing these 3 checks, if necessary, notification could then be made to the appropriate staff or engineers as required.

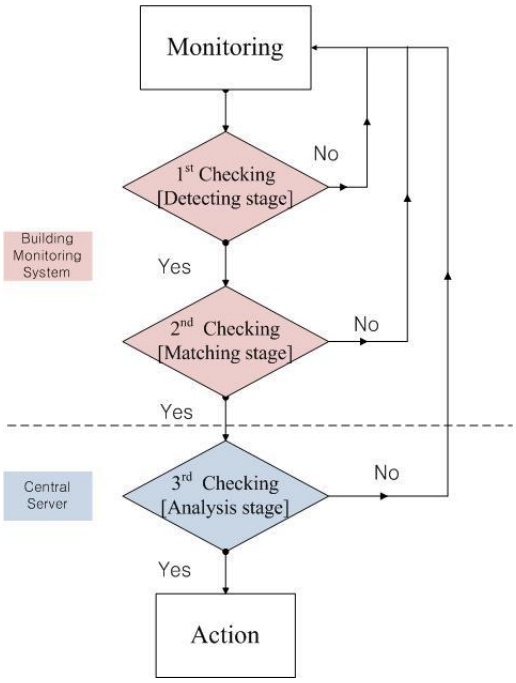

Figure 14: Proposed Fault Diagnostic Flow Chart

There is also scope for this system to be implemented in the sustainable container unit as the discussed potential CM system. It was felt that a this system would could be useful as consideration was being made to transferring this to a commercial building and it would ensure operational costs were kept to a minimum while further aiding to increase reductions of grid supplied power due to maximum operational times of any sustainable devices installed. This system was seen as beneficial as typical condition monitoring techniques are usually either too expensive or impractical in size when considering their use in conjunction with micro renewables. Methods such as monitoring of oil samples, measuring stresses on blades, vibration and acoustic analysis of bearings in the case of wind turbines and Thermography and other such methods in the case of PV, all require a number of sensors which would be impractical and increase both cost and potential maintenance for both the navigation buoys and the container unit. Instead the research focused on developing cheap methods of monitoring performance and identifying any trends in failure of performance of each renewable generator so as to fit with the proposed fault flow path in Figure 14.

This is the area of research was under taken a visiting student at the University Of Strathclyde as part of the joint research project through the ESRU research group and it was intended that this project be combined with the research from this Thesis for further development of the final system.

The intention was to develop an understanding of the performance of PV panel's under varying operating conditions. This would then lead to the development of trend analysis data that could be used for the development of fault algorithms. These algorithms could then be implemented within the Java application in the 1st stage of fault identification and would be based on electrical performance parameters which are easy and cheap to monitor in respect to the overall cost of the generators themselves.

5. Experimental Research

5.1 Methodology

The main research towards this Thesis on power optimisation was to gain an understanding of the impact on the overall efficiency of these PV panels when connected to a load without MPPT. The panels used in the research were the same as those used in both the buoy and container unit research projects however the main focus was on the panels integrated with the buoys. To begin with a basic methodology was defined. This took the form of a flow chart as can be seen in Figure 15 below:

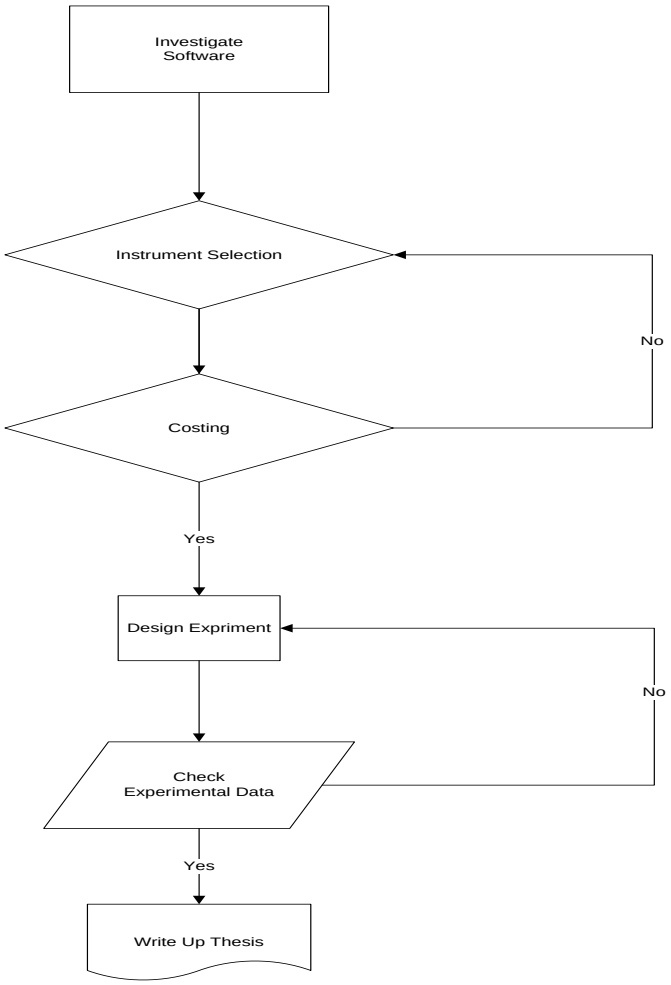

Figure 15: Research Work Flow

The 1st step was to gain familiarity with the software interface, LabVIEW, which would be used to retrieve data from the experiment, display it in real time and record it for further processing. As part of this process a number of basic tutorials were completed so as to gain an understanding of how the programme operates and a few of its many uses. At this point a basic 1st stage design for a potential interface was created.

The next step was to select the required sensors. Considerations were made for the measurable environmental parameters that would impact the overall performance of the PV panels. Cost was then assessed to ensure it was minimal in comparison with the capital required for the PV panels themselves. Also taken into consideration was whether or not the chosen instruments would be useful for potential condition monitoring processes so as to help in the development of this part of the project and any CM algorithms that may be produced.

The next step was to confirm the design of the virtual instrument to be used in LabVIEW. It had to be able to convert the sensors output signals into a recognisable SI unit, display this information in real time and also create a copy of the for further analysis after the experiment was complete. Each sensor was then connected up to the computer and calibrated to ensure outputs were displayed correctly and were of a reasonable level of accuracy.

Once the VI was completed and the sensors correctly calibrated, the PV panels were installed in a small light bed already in place in the lab and measurements taken. Over a period of time of the panel temperature and levels of solar radiation were varied and the electrical outputs recorded, this data was then used in the final analysis.

5.2 Instruments and Equipment

In developing this experiment to analyse the PV system the 1st step was in deciding how best to collect any data that might be recorded. It was decided that the best option was to use a PC based application. LabVIEW was chosen as it allows for an intuitive interface to be used to control a more complex underlying program. With the number of sensors we expected to be using it also allowed for these to be connected up to one PC and for the data to be gathered at one single point rather than using a number of other instruments to collect data to separate points and then have to collate this all together after every single run of the experiment.

In considering the choice of instruments that would be used to gather the required data it was decided to use a small thermocouple to monitor directly the panel temperature, a small photodiode was chosen to measure the amount of light incident on the panels and an ambient temperature and humidity sensor was chosen to measure the surrounding air temperature for a comparison to the panel temperature.

Once the sensors were calibrated and connected to the pc the next step was to set up the monitoring of the electrical properties of the system in order to create a comparison of them to the measured environmental conditions. This was done by connecting the panel to a small 5Ω resistor and the voltage across this and the current through it. Again this information was calibrated to ensure the LabVIEW program was displaying correctly measured values. Details of the LabVIEW program and instruments used can be found on the following pages.

5.2.1 LabVIEW

LabVIEW is a graphical programming environment, an application created by National Instruments, which can be used to create control systems and test systems and in this case allows measured data to be easily recorded. The system has been designed to receive external electrical inputs from the sensor equipment for the experiment on a PC in the lab. This allows the signals received to be processed and displayed in real time while also being recorded and output to a text file for further analysis. It implements predefined Virtual Instrument's (VI's) which have been selected and matched up as appropriate.

LabVIEW provides to displays of any interface it used to design the block diagram shown here in Figure 16 and the front panel which is the direct graphical user interface and is shown in Figure 17

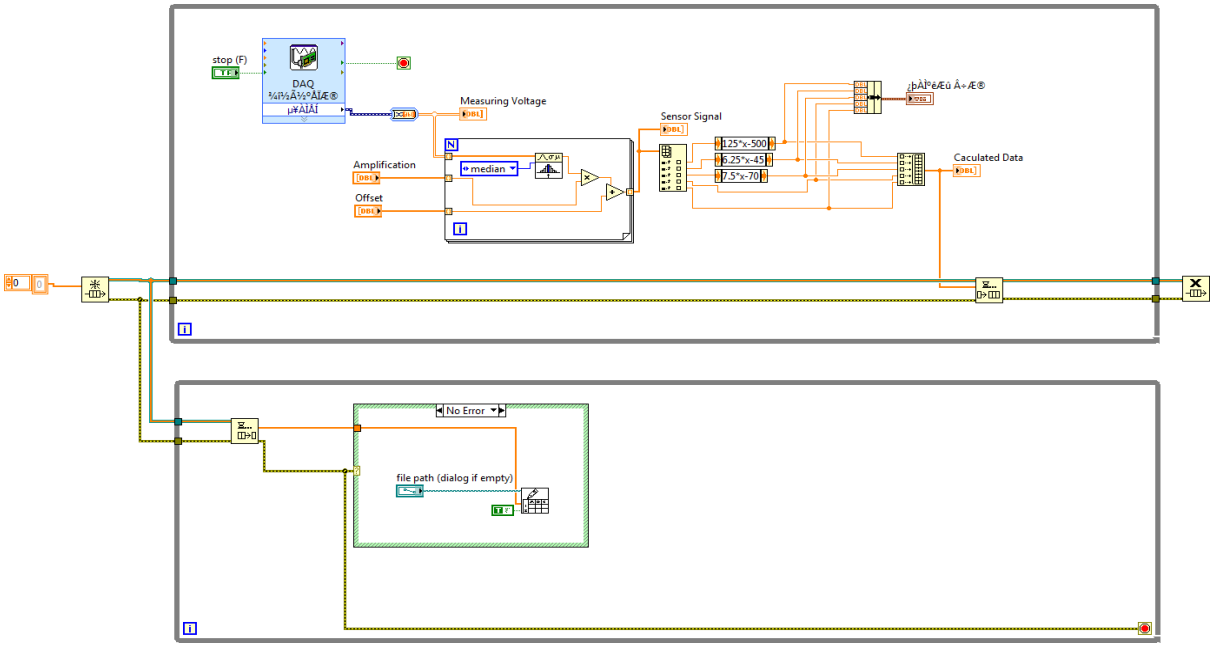

Figure 16: LabVIEW Block Diagram (Screen Shot)

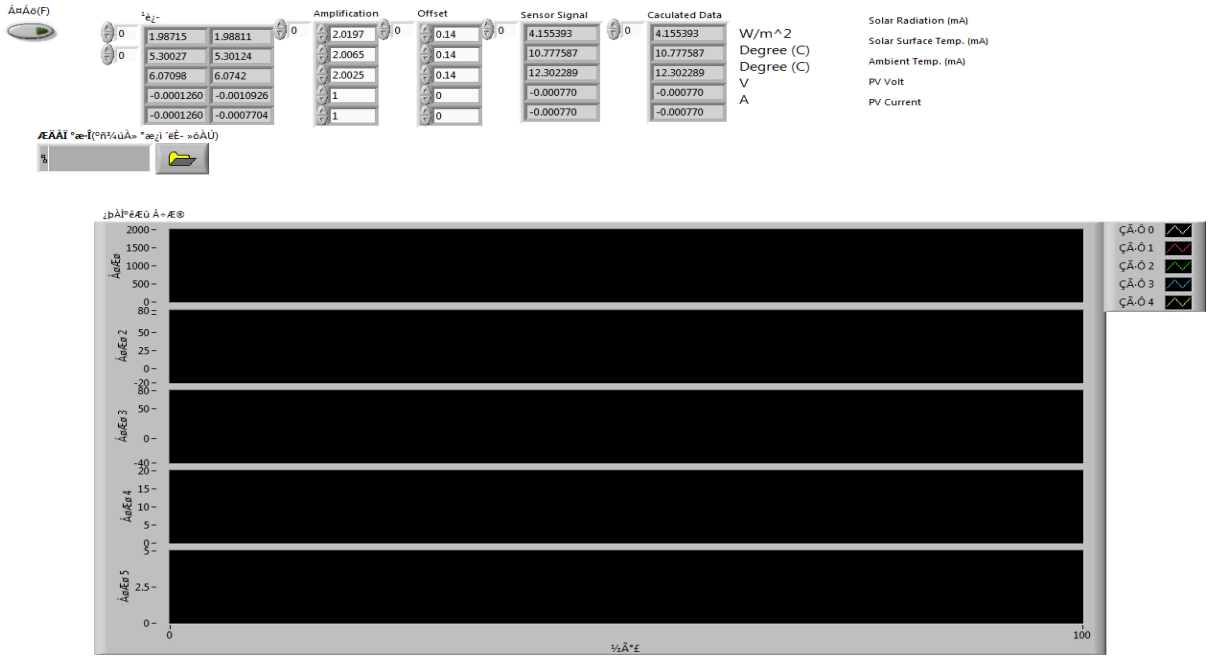

Figure 17: LabView User Interface (Screen Shot)

In this instance program was designed to record data received by a DAQ interface (Figure 16) from a number of inputs including each of the sensors and the PV panel set up. Each sensor is connectd to a bread board (Figure 17) which was wired to convert to all output signals to acceptble voltages to be input to the DAQ card with in the lab PC. This DAQ card allowed for the small VI created within LabVIEW to record voltage and current levels during each run of the experiment. The voltage of the PV panel was stepped down from 40 to 10V using a 3:1 resistor circuit. Current and voltage values were calculated by measuring the levels across and through a 5Ω resistor load. This data was fed into the DAQ device through a small terminal board (Figure 18).

Initially 10,000 samples were taken for each input over 1 second. Once the data was recevied by the DAQ device it was passed on to the VI for processing. The mean of the data for each input was calculated and taken to be the value at that instant. This data was then processed with offset and amplification data calculated through measurment and converted from an electrical value into it's scientific value equivalent ie Wm¯2. This was information was then dispalyed on the front end view for the user to view. At the same time it was also written to text files for storage and a file in file out (FIFO) loop was built into to wipe the stored data from the computer memory once this was completed to ensure optimal operating of the machine.

Figure 18: DAQ

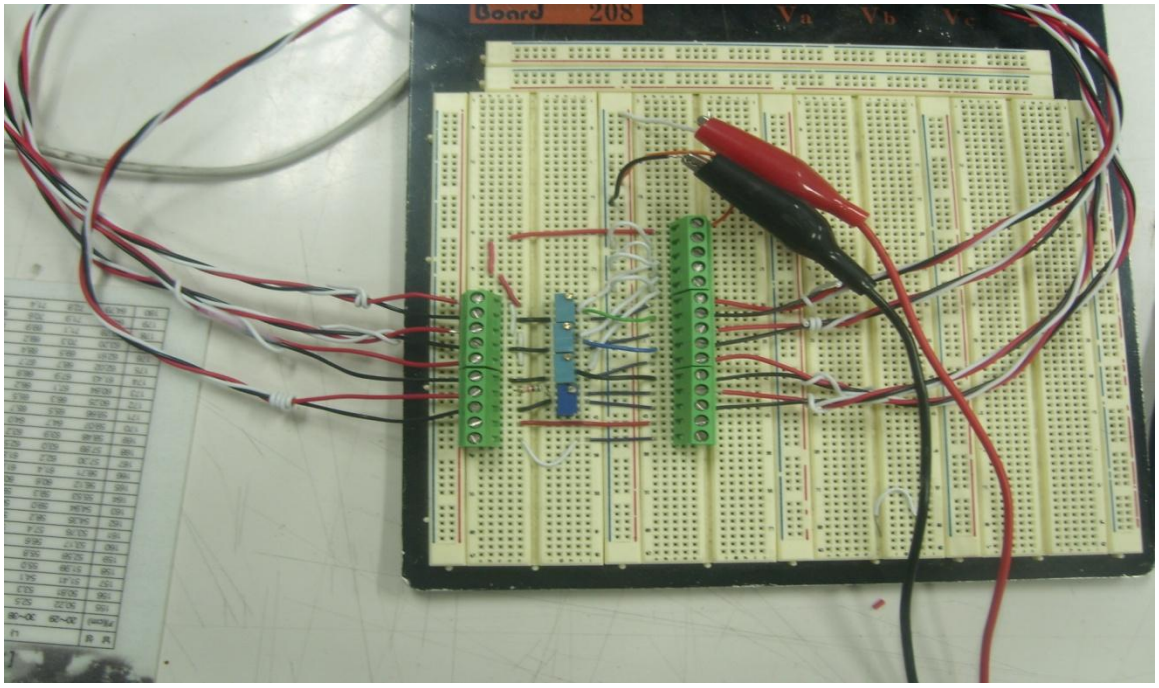

Figure 19: Bread Board

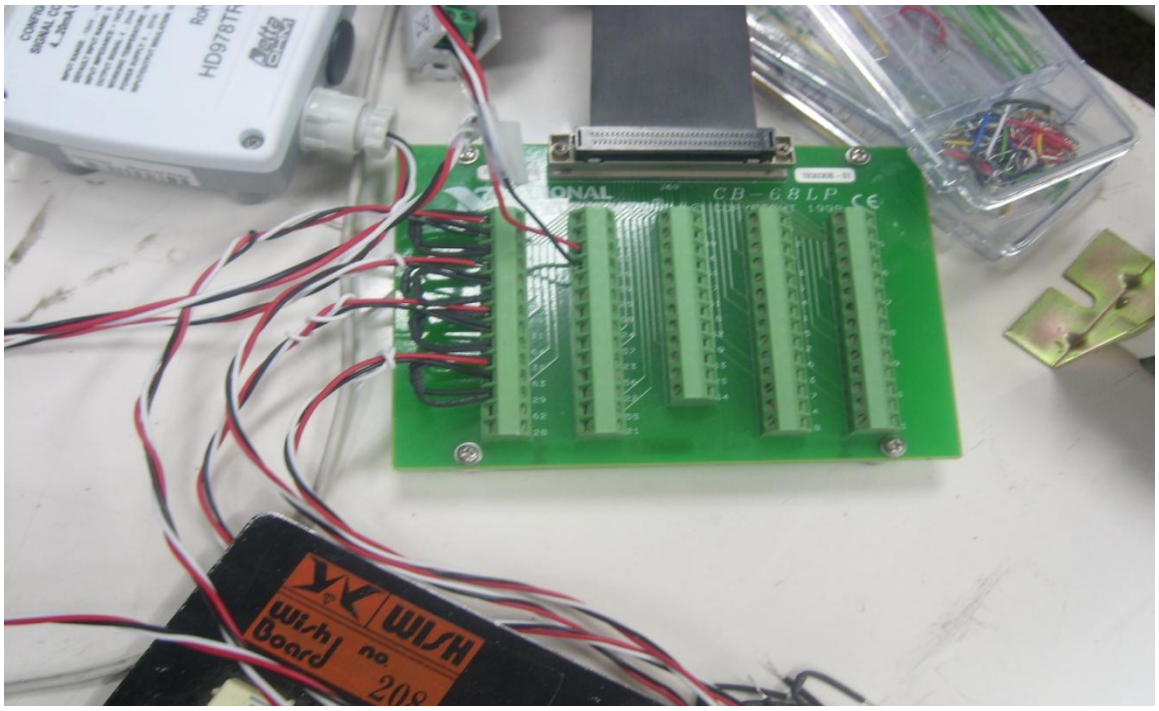

Figure 20: Terminal Board

5.2.2 Thermo-couple

A small thermocouple (Figure 21) was chosen to measure the surface temperature of the PV panel. It was positioned on the rear of the panel in the centre and attached using a thermal paste to ensure optimal thermal bridging between the sensor and the panel surface. Normally a number of sensors would be used to measure the temperature flux across the surface of the panel but as the aim one of the aims of this project was to minimise costs it was decided to use a single sensor.

The thermal sensors measures range of temperatures is between -20^{o}C and 80^{o}C. The electrical output range of the sensor is between 4 and 20mA. The VI was calibrated to convert this output from mA into ^{o}C.

Figure 21: Thermocouple

5.2.3 Ambient Temperature Sensor

It was decided to use an ambient air and humidity sensor as although humidity may not affect the PV performance it may have an effect on the wind turbine output and as there is scope for the sensors to be used in conjunction with CM it was felt this was the best choice. In the case of this experiment the sensor was only used to measure the air temperature in comparison with the temperature of the PV panel as any major deviation from expected temperature differences may indicate fault development. It was placed directly between the panels and light source so as to measure the air gap between the 2 as this would be heated above room temperature by radiation absorbed from the bulbs.

Figure 22: Ambient Air and Humidity Sensor

Figure 23: Sensors

5.2.4 Halogen Light bulbs

The light bulbs used in the light bed were 50 watt halogen lights. There were a total of 75 bulbs, (5x15) These bulbs emit in the range of between 400 and 1000nm as can be seen in the graph below (Figure 24):

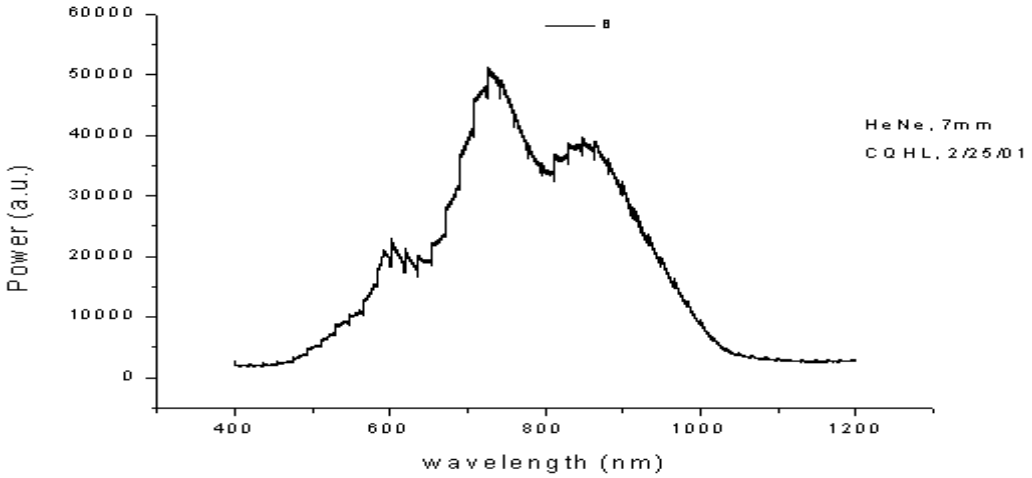

Figure 24: Halogen Spectral Emission

This is well suited to silicon which has a spectral response that sits in the range of between 300nm and 1200nm (Figure 25):

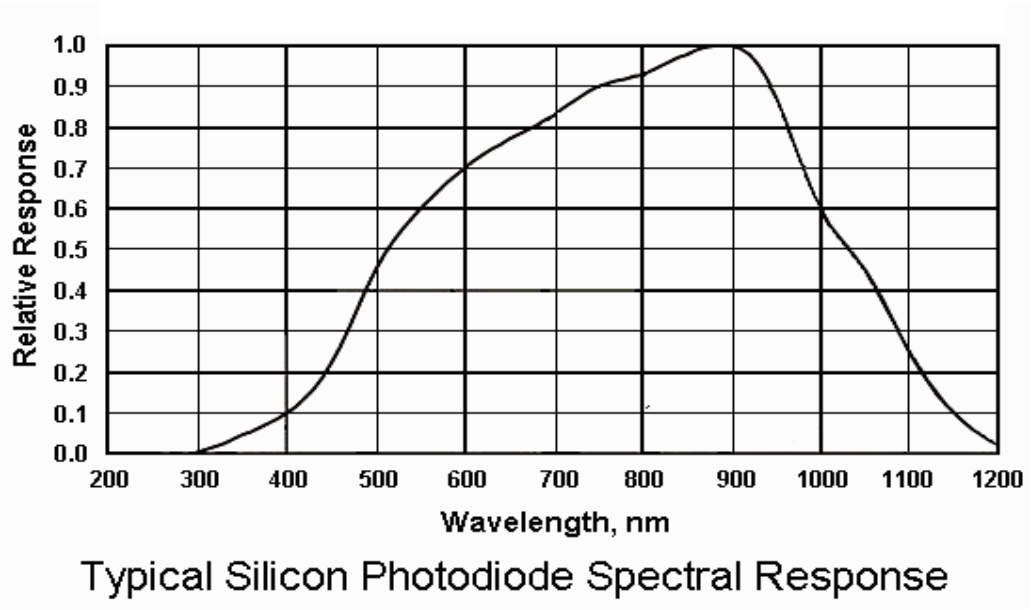

Figure 25: Silicon Spectral Response

The bulbs were set approximatly 45cm above the panels shinning down. They were spread out so as to give as even as possible a spread of light across the PV panels (Figure 26, not the final set up but an initial configuration). This was as to ensure maximum response from each cell with in the panel.

Power to the light bulbs was controlled through a variable resistor between them and the mains power supply.

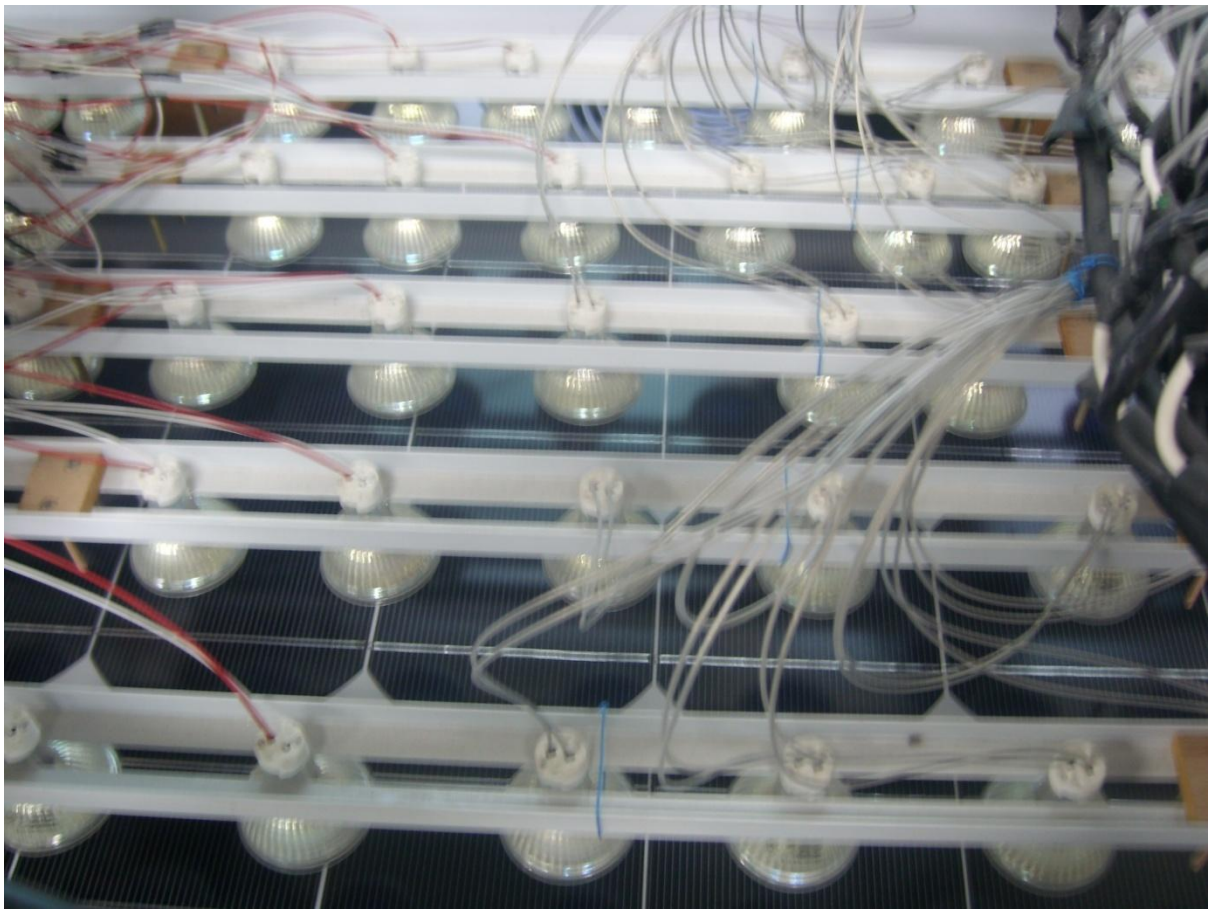

Figure 26: Light Bed

5.2.5 Photodiode

The photodiode device selected measures between 400nm and 1000nm EM radiation. The signal is output at 2.6µV/Wm^{-2} and this was used to calibrate the voltage output into W/m^{-2} in the VI. A photodiode sensor was chosen over a pyronometer as it was significantly cheaper and its spectral response range was well matched with the spectral response of the silicon panel and the spectral emissions of the halogen light bulbs.

During the experiment the sensor was placed in alignment on the horizontal and vertical planes with the PV panel to measure the total incident solar radiation.

Figure 27: Photodiode

5.2.6 PV Panels

The PV panels used in this experiment were 60W polycrystalline with a maximum voltage V_{max} of 20.4V and a maximum current I_{max} of 2.94A. During the experiment one cell was tested individually and then 2 were tested in series as was the setup of the panels on both the container unit and navigation buoys.

Figure 28: PV Panel

In order to be able to measure the changes in voltage and current produced by the PV panel, 2 separate wires were soldered to the positive and negative contacts. These were then connected to a 5Ω load and on to the bread board, through a terminal board and into the NI DAQ card installed on the PC in the lab.

5.3 Calibration

To insure accuracy of results, the sensors used had to be calibrated to ensure their output values displayed on the VI were equivalent to actual voltage and readings taken from each sensor along with the outputs of the PV panel.

The 1st step was to calculate offset values for each sensor along with voltage and current outputs from the panel. To calculate this figure the actual output from each sensor was measured with a multi meter and a zero value of each output from PV panel, thermocouple and solar radiation sensor were recorded when there was no incident radiation and no increase in temperature above that of the ambient climate. These values were compared with the onscreen value displayed on the LabVIEW VI and any difference taken to be the offset value.

To calculate any amplification of the signal that may have been required several different levels of voltage were recorded and compared with on screen values starting with the maximum output value and working down progressively. This is done for several values and, to calculate the amplification required, the difference of each voltage recording and its display equivalent were noted, added together and the average taken to be the required amplification. This process was repeated twice for each measured value and the average used as the final figure.

Finally to ensure these calibration figures provided reasonable results they were compared to real world values measured and a number of samples compared to ensure a minimum variation of +/- 5% of the actual real world value as this was deemed to be of an acceptable tolerance level.

5.4 Experimental Setup and Procedure

5.4.1 Setup

To begin with it was decided that a light bed already in place in the E2E lab would be used to test the photovoltaic panels. This consisted of a large frame of dimensions 1.3m by 0.55m. This means the amount of power emitted works out to be approximately 5.24kWm^{-2}. As the panels in use were silicon based this also meant there was no need to change the bulbs as the spectral emissions matched the silicon spectral response as mentioned before. It was decided then that all data would be recorded on a PC with the LabVIEW interface. Once the sensors had been selected and calibrated the one of the panels was installed in the light bed. It was hung 45cm from the light source so as to allow for adjustments at a later stage. The thermocouple was already in place, the ambient air sensor was positioned in the air gap between the panel and lights. It was fixed to one of the legs of the frame and set at a vertical position as required. Finally the photodiode was placed on a small metal rail in alignment with the PV panels directly under the light source. The system was already wired up as discussed.

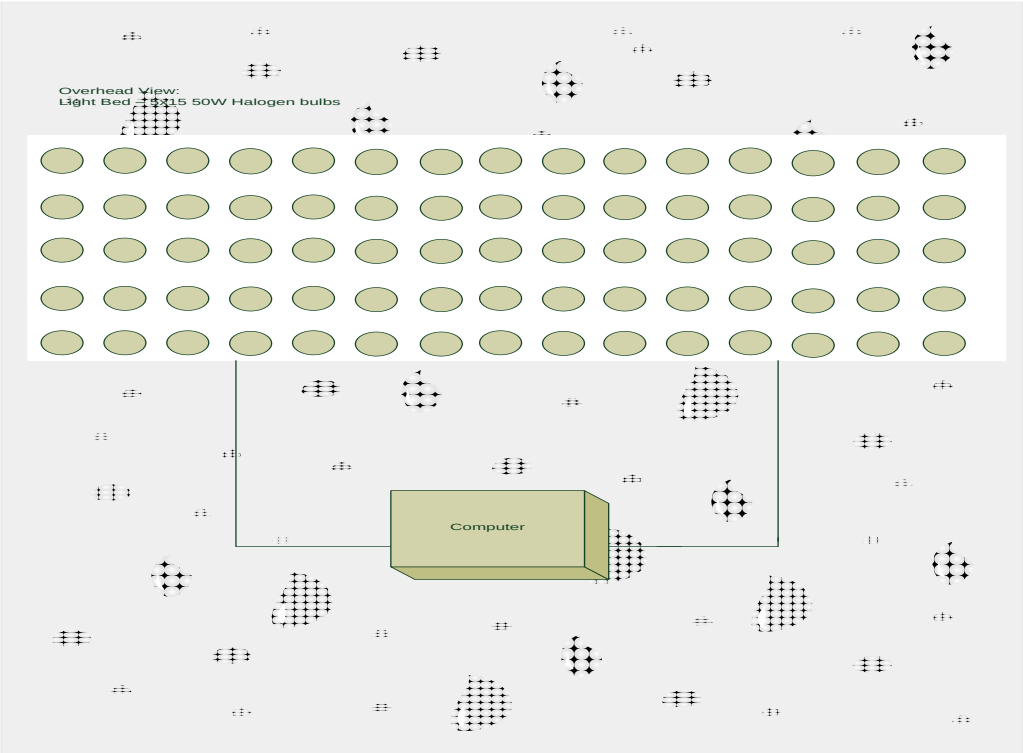

Figure 29: Proposed Experimental Layout

5.4.2 Procedure

Once all instruments were in place and the VI program correctly configured a single panel was placed under the light bed. The VI program was set to record and the light bed turned up to full power to illuminate the Panel. Power to the light bulbs was controlled through a sliding resistor control unit which allowed voltage input to be changed from 0 to 240V. Temperature and direct solar radiation levels were both recorded with temperature increasing over time and solar radiation maintaining a constant level.

Due to limits in the operating temperature of the thermocouple used, it was decided to limit the upper temperature of the experiment. The thermocouple operating range was from -20oC to a maximum temperature of 80oC. The length of time for the panel to heat to over 70oC was noted and it was decided this would be how long each experiment was run for as. This was found to be 30 minutes and so the system was set to run for 1800s stopping the recording after this time and the LabVIEW program was designed so as to emit a tone to confirm it had finished a cycle.

At this point the panel was allowed to cool and the experiment was repeated to confirm the results. The next step was to connect the panel in series with a 2^{nd} one and see how performance differed, if there were any significant losses and what the overall power output was.

6. Results

6.1 Constant Solar Radiation

6.1.1 Single Panel

Over a temperature range of 27^{O}C to 73^{o}C and under 255 Wm^{-2} of solar radiation, a single polycrystalline panel saw a drop in performance from 22.8W instantaneous power to 16W this equates to a loss of 29.8% *Figure 30* and a drop in conversion efficiency from 8% to 6% .

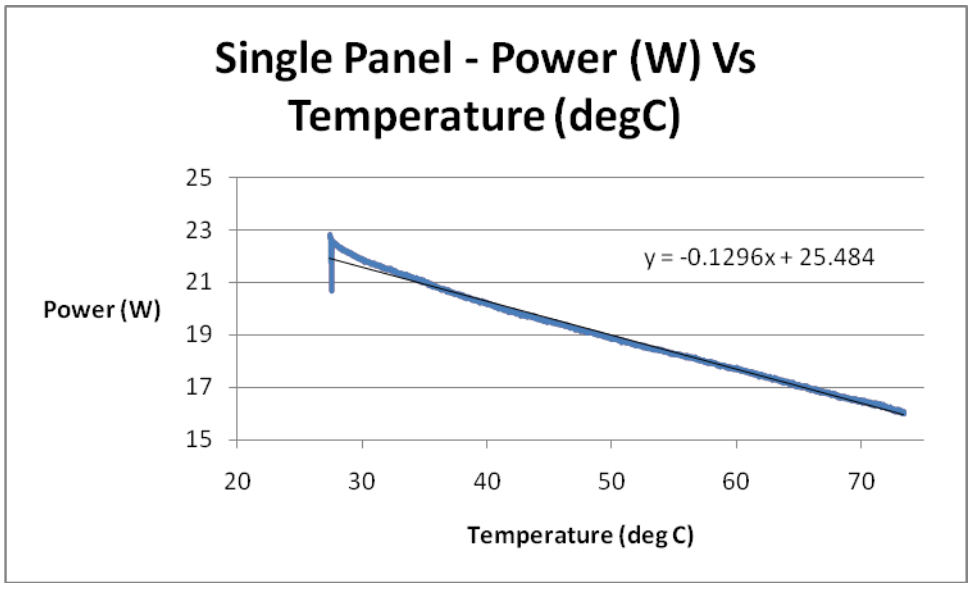

Figure 30: Single Panel, Change in Power with increasing temperature

6.1.2 Two Panels in Series

Looking at 2 panels connected in series over the same temperature range of 27 – 73^{o}C under constant solar radiation levels of 255Wm^{-2}, the maximum power at 27^{o}C was 41.9W dropping to 33.1W at 73^{o}C. This equates to a loss in performance of 21% (*Figure 31*)

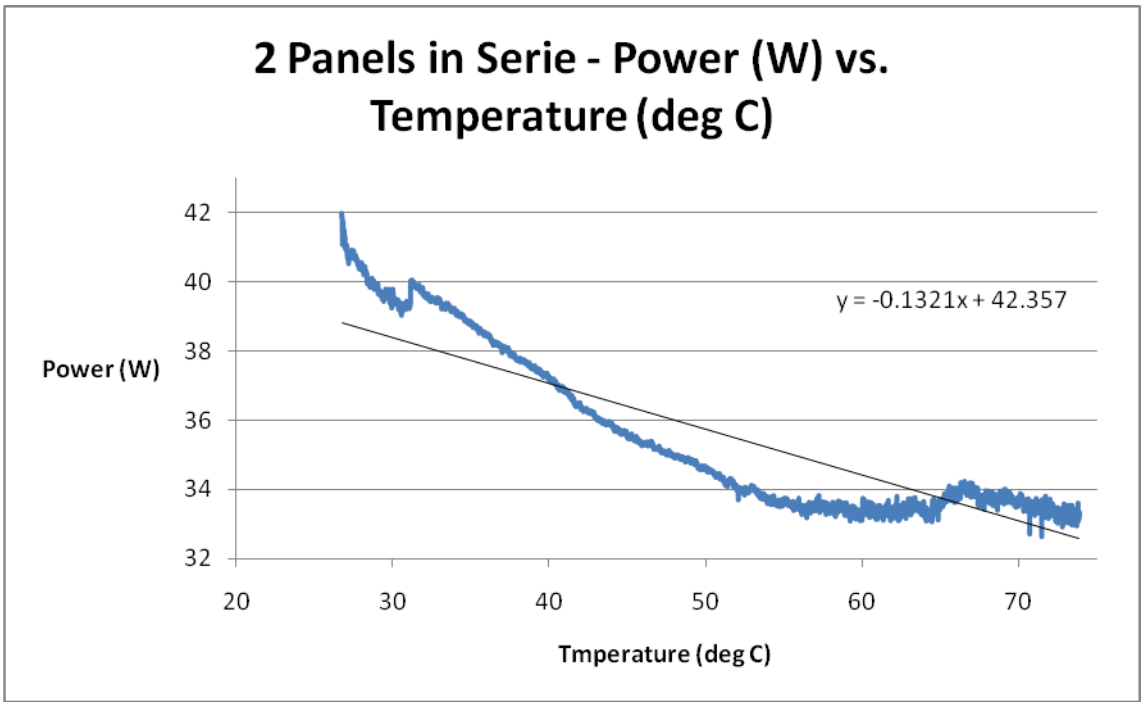

Figure 31: 2 Panels in Series Change in Power with Increasing Temperature

As expected a drop off in performance can be seen as temperature is increased. Comparing the single panel performance with 2 cells in series, it would be expected that the 2 panels in series would produce closer to twice the power of the single panel 45.6W. In fact there would appear to be a drop in performance of around 8%, much more than could be attributed to losses due to increased resistance in the circuit.

Looking at *Figure 30 and 29* the loss in power in the single cell is almost linear where as the loss in power in the 2 panels in series is very erratic. This would suggest a potential fault with the 2nd cell. A closer inspection of voltages produced by the 2 panels in series against those produced by the single panel highlights a non-linear drop in voltage influencing the shape of the output power *Figure 32*:

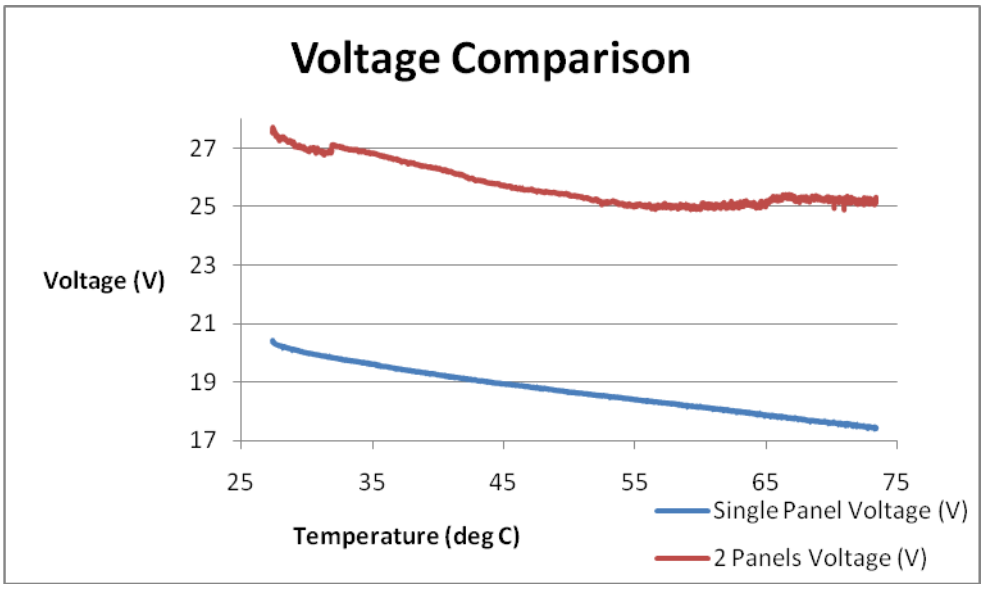

Figure 32: Comparison of Voltages

6.2 Constant Temperature

6.2.1 Single Panel

As can be seen in *Figure 33* there is a steady increase in power produced with increasing incident solar radiation (quantified here as Wm^{-2}) with very little impact in the output power over a range of $10^{o}C$. As shown in section 6.1 for significant loses to be seen measurements need to be taken over a large temperature range.

Looking at the opposite ends of Figure 31 it can be seen regardless of incident solar radiation, conversion efficiency stays the same. Under 110 Wm^{-2} and at $25^{o}C$ the panel converts 9.5% and at 230 Wm^{-2} under $25^{o}C$ it converts 10%, a shift of 0.5% over a range of 120 Wm^{-2}

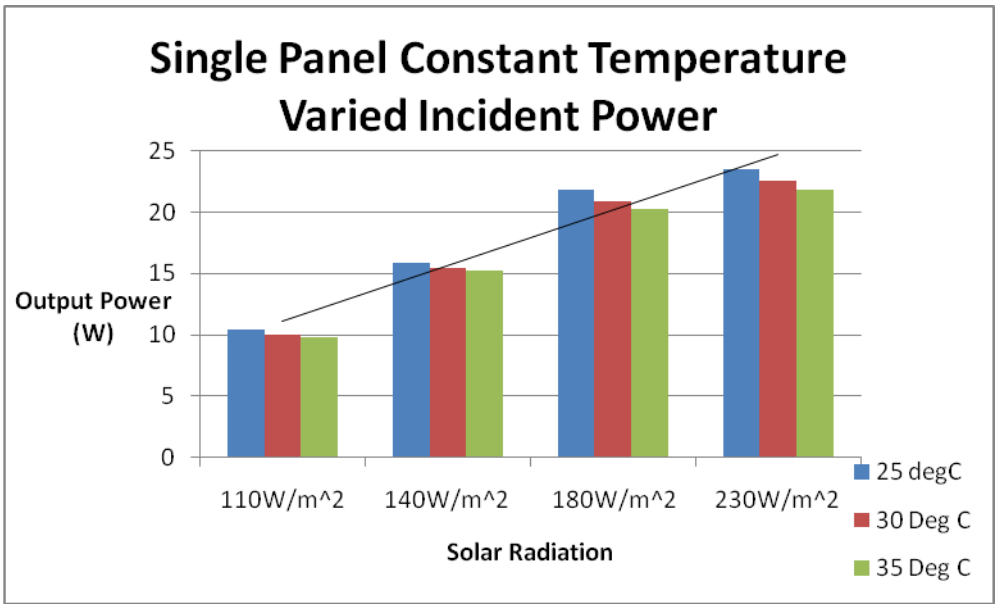

Figure 33: Constant Temperature, Increasing Solar Radiation

6.2.2 Two Panels in Series

Looking at the performance of the panels in series again there is a slight anomaly in the power output. Looking at the output power at 110Wm^{-2} it is the same as the output of a single panel however at the higher levels of irradiance the panels appear to perform as under the first experiment. This would seem to point towards an issue in the panel's ability to begin generating at lower levels of solar radiation.

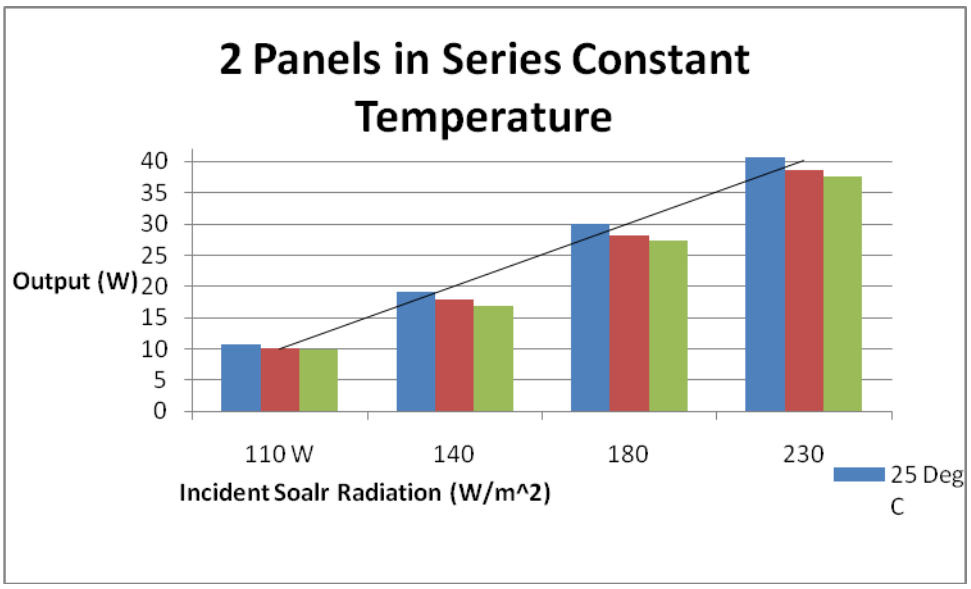

Figure 34: 2 Panels In Series Constant Temperature

It should be noted that due to limitations in the ability to vary supply voltage to the light bed that the stepped increase in power is not totally linear however the experiment still. Also due to the nature of the experiment lower energy outputs restricted the temperature rang the 2nd experiment could be performed over.

7. Discussion

7.1 Maximum Power Point

In considering the performance of the PV panels in this experiment the results looked at their overall performance with respect to environmental conditions. In order to consider how their performance could be optimised with respect to the maximum power point at a specific temperature or under specific amounts of solar radiation we first need to know the fill factor of the panel. From eq 6 we can see this is the ratio of V_{max} and I_{max} to V_{oc} and I_{sc}. In the case of this panel this gives a value of 0.52, where V_{oc} was found to be 22.01V and I_{sc} was found to be 5.2, experimentally.

Re-arranging eqn 6 we can then easily find what the maximum power should be for any known V_{oc} and I_{sc} at any temperature (eqn 8) and thus asses what the maximum power should be and therefore how well the PV panel is performing over temperature:

$$MPP = FF\, V_{oc}\, I_{sc} \quad (8)$$

Temperature (Deg C)	VOC (V)	ISC (A)	MPP (W)	Actual Power (w)
25	22.01	5.2	59.51	23.517
30	21.57	5.1	57.2	22.533
35	21.14	5.04	55.4	21.803

Figure 35: MPP Table

Figure 34 above shows the values of V_{oc} and I_{sc} temperatures of 25, 30 and 35^{o}C and compares the MPP value with the actual power generated during testing. Without the use of MPPT there is a drop in conversion efficiency of around 60%.

7.2 Improvements

In considering the results gained from this experiment, areas that could be improved and expanded upon include a more controlled investigation of the thermal impact on the PV panel array. In this experiment the heating from the light source itself was relied upon. If this were controlled more it might allow for an increased range of results to give a more detailed profile of the performance of a panel with constant solar radiation levels.

Implementation of a pyranometer within the experimental setup might also help in giving more detailed information on the range of solar radiation incident on the solar panels and give better understanding of how close to real world performance the lab experiment is.

An increased number of thermocouples to measure panel surface temperatures might also be useful. This would help to develop an idea of any temperature gradients across the panel and identify any areas of potential fault such as in the 2nd panel.

7.3 Further Research

Some areas of further research that are required to improve and expand upon the data in this experiment include a cost benefit analysis. This would need to look at the overall cost of implementing MPPT and CM systems against the cost, per kWhr, of conventionally grid drawn energy. This would also need to factor in the newly introduced fed in tariff as any excess energy at present has the potential to off-set expenditure.

Repeating this experiment with a different panel could prove useful in confirming the performance characteristics and ensure any CM system is robust and able to be implemented on any panel type so as to improve any potential uptake.

It may well be worth investigating the root cause of the fault within the 2nd panel used in these experiments. Initially this appeared to be a problem however it highlights the kind of problems that can occur due to faults in such devices and could be an advantage in the case of developing the algorithms required for a CM system. Once understood it could provide the 1st fault profile or be a very good test component of the system.

The next stage of this research is to look into the development of these specific algorithms for implementation in CM system. The data produced here is intended to provide the base performance information upon which algorithms might be developed from. It is likely these will come from the relationship between the V_{out} and V_{oc}, however for the 2nd and 3rd stages more detailed weather based performance data and data based on comparison of cell performance would be required.

8. Conclusion

In considering the results obtained from this thesis it is clear that MPPT is of vital importance in ensuring optimal performance of any PV array. Even in the case of this small set-up, a single 60W panel so losses of 60%. Although it has been shown that a well matched load can negate the need for such a system, in an environment such as the sustainable container unit where cooling demands may vary it is clearly not going to suit such a set up.

In fact in most domestic or business settings where demand is very dynamic it is unlikely that the removal of MPPT as a method of cost saving is likely to be justifiable. This is especially the case now with the introduction of the feed in tariff for unused sustainably generated electricity meaning any excess power could be seen as an income to offset this initial expenditure.

Where it still might be justifiable is in medium sized industrial sites where they may not be entitled to claim FIT's or see the full benefit and may also have a more predictable, relatively static, constant load such as a refrigeration system or in a chemical processing plant or manufacturing line.

However it is looked at, it is clear, as we move to a more distributed, sustainably generated energy society, with ever increasing demands in energy consumption, power optimisation of one sort or another will be necessary to ensure as much energy as possible is extracted from these resources as well as other renewable sources such as wind and hydro.

With ongoing developments in the semiconductors used to create PV panels and promises of up to 60% efficient cells (http://www.bbc.co.uk/news/science-environment-11095650) and even research into the use of chlorophyll, the chemical associated with photosynthesis, (Wang et al. 2010) it is clear there is a bright and energetic future for photovoltaic's and renewable generation as a whole.

References

International Energy Agency, World Energy Outlook 2008

Feed-in Tariffs Government's Response to The Summer 2009 Consultation

The U.K. Energy Act 2004 pg65 Section 82(7-8)

Birkmire, R.W. & Eser, E., 1997. Polycrystalline thin film solar cells: present status and future potential. *Annual Review of Materials Science*, 27(1), 625–653.

Braga, A. et al., 2008. New processes for the production of solar-grade polycrystalline silicon: A review. *Solar Energy Materials and Solar Cells*, 92(4), 418-424.

de Brito Filho, J.P. & Henriquez, J.R., 2010. Infrared thermography applied for high-level current density identification over planar microwave circuit sectors. *Infrared Physics & Technology*, 53(2), 84-88.

Dasgupta, N., Pandey, A. & Mukerjee, A.K., 2008. Voltage-sensing-based photovoltaic MPPT with improved tracking and drift avoidance capabilities. *Solar Energy Materials and Solar Cells*, 92(12), 1552-1558.

Dubey, S. & Tiwari, G., 2008. Thermal modeling of a combined system of photovoltaic thermal (PV/T) solar water heater. *Solar Energy*, 82(7), 602-612.

Firatoglu, Z.A. & Yesilata, B., 2004. New approaches on the optimization of directly coupled PV pumping systems. *Solar Energy*, 77(1), 81-93.

Fraisse, G., M[illegible]o, C. & Johannes, K., 2007. Energy performance of water hybrid PV/T collectors applied to combisystems of Direct Solar Floor type. *Solar Energy*, 81(11), 1426-1438.

Jahanshah, F. et al., 2009. pn Junction depth impact on short circuit current of solar cell. *Solar Energy*, 83(9), 1629-1633.

Jain, S. & Agarwal, V., 2007. New current control based MPPT technique for single stage grid connected PV systems. *Energy Conversion and Management*, 48(2), 625-644.

Kar, C. & Mohanty, A., 2006. Monitoring gear vibrations through motor current signature analysis and wavelet transform. *Mechanical Systems and Signal Processing*, 20(1), 158-187.

Konovalov, I.E., Breitenstein, O. & Iwig, K., 1997. Local current-voltage curves measured thermally (LIVT): A new technique of characterizing PV cells. *Solar Energy Materials and Solar Cells*, 48(1-4), 53-60.

Kostic, L.T., Pavlovic, T.M. & Pavlovic, Z.T., 2010. Influence of reflectance from flat aluminum concentrators on energy efficiency of PV/Thermal collector. *Applied Energy*, 87(2), 410-416.

Mann, M.E., Bradley, R.S. & Hughes, M.K., 1998. Global-scale temperature patterns and climate forcing over the past six centuries. *Nature*, 392(6678), 779–787.

Markvart, T., 2003. *Practical handbook of photovoltaics : fundamentals and applications*, New York: Elsevier Advanced Technology.

Mazer, J., 1996. *Solar cells : an introduction to crystalline photovoltaic technology*, Boston: Kluwer Academic Publishers.

McIntyre, S. & McKitrick, R., 2003. Corrections to the Mann et. al.(1998) proxy data base and northern hemispheric average temperature series. *Energy & Environment*, 14(6), 751–771.

Möller, H., 1993. *Semiconductors for solar cells*, Boston: Artech House.

Neamen, D., 2003. *Semiconductor physics and devices : basic principles* 3rd ed., Boston: McGraw-Hill.

Norton, B. et al., Enhancing the performance of building integrated photovoltaics. *Solar Energy*, In Press, Corrected Proof. Available at: http://www.sciencedirect.com/science/article/B6V50-4Y82NB9-1/2/509b61ff23b14fd48ee70cd15c76be4c.

Wang, X. et al., 2010. Significant enhancement in the power-conversion efficiency of chlorophyll co-sensitized solar cells by mimicking the principles of natural photosynthetic light-harvesting complexes. *Biosensors and Bioelectronics*, 25(8), 1970-1976.

Woditsch, P. & Koch, W., 2002. Solar grade silicon feedstock supply for PV industry. *Solar Energy Materials and Solar Cells*, 72(1-4), 11-26.

Yu, G.J. et al., 2004. A novel two-mode MPPT control algorithm based on comparative study of existing algorithms. *Solar Energy*, 76(4), 455-463.

Appendix A

Open Circuit Voltage Data:

25.197	22.01371
25.674	21.98971
26.205	21.96571
26.762	21.91314
27.301	21.86057
27.816	21.83771
28.312	21.81486
28.829	21.75543
29.385	21.696
29.953	21.63771
30.537	21.57943
31.028	21.54514
31.542	21.51086
32.032	21.45714
32.579	21.40343
33.14	21.33943
33.681	21.27543
34.212	21.25257
34.681	21.22971
35.181	21.14743
35.697	21.06514
36.237	21.04229
36.75	21.01943
37.242	20.99543
37.666	20.97143
38.148	20.91886
38.593	20.86629
39.065	20.808
39.553	20.74971
39.977	20.72571
40.452	20.70171
40.875	20.66743
41.291	20.63314
41.765	20.57371
42.167	20.51429
42.585	20.49714
42.985	20.48
43.319	20.44457
43.698	20.40914

44.184	20.36229
44.565	20.31543
44.892	20.29257
45.208	20.26971
45.564	20.24
45.952	20.21029
46.296	20.16914
46.704	20.128
47.008	20.09943
47.272	20.07086
47.6	20.06514
47.904	20.05943
48.296	20.01257
48.544	19.96571
48.872	19.94743
49.144	19.92914
49.464	19.912
49.752	19.89486
50.04	19.85371
50.384	19.81257
50.584	19.80114
50.752	19.78971
51.024	19.77829
51.304	19.76686
51.56	19.72
51.912	19.67314
52.112	19.66057
52.272	19.648
52.48	19.63657
52.8	19.62514
53.008	19.59657
53.28	19.568
53.432	19.55543
53.616	19.54286
53.808	19.53714
54.024	19.53143
54.288	19.50286
54.504	19.47429
54.672	19.456
54.736	19.43771
54.92	19.43771
55.136	19.43771
55.344	19.39657
55.512	19.35543
55.688	19.35543
55.8	19.35543

55.976	19.34971
56.128	19.344
56.312	19.32114
56.496	19.29829
56.672	19.28686
56.752	19.27543
56.944	19.28114
56.976	19.28686
57.152	19.25143
57.32	19.216
57.432	19.20457
57.6	19.19314
57.68	19.19886
57.856	19.20457
57.952	19.17486
58.16	19.14514
58.288	19.13943
58.36	19.13371
58.424	19.13371
58.536	19.13371
58.68	19.11657
58.808	19.09943
58.912	19.088
59.056	19.07657
59.072	19.088
59.184	19.09943
59.352	19.05829
59.456	19.01714
59.52	19.01714
59.608	19.01714
59.696	19.02857
59.784	19.04
59.984	19.00571
60.048	18.97143
60.12	18.96457
60.152	18.95771
60.192	18.96457
60.352	18.97143
60.512	18.95886
60.552	18.94629
60.68	18.92914
60.704	18.912
60.776	18.92914
60.848	18.94629
60.968	18.912
61.056	18.87771

61.112	18.88343
61.288	18.88914
61.248	18.90057
61.296	18.912
61.36	18.888
61.44	18.864
61.576	18.84114
61.6	18.81829
61.584	18.84114
61.672	18.864
61.776	18.84114
61.888	18.81829
61.936	18.81829
61.944	18.81829
62.024	18.83543
62.136	18.85257
62.12	18.82971
62.264	18.80686
62.304	18.78286
62.288	18.75886
62.408	18.78857
62.44	18.81829
62.608	18.78286
62.68	18.74743
62.712	18.75314
62.768	18.75886
62.736	18.77143
62.8	18.784
62.872	18.76
62.984	18.736
62.992	18.73029
63.072	18.72457
63.112	18.736
63.168	18.74743
63.24	18.72457
63.408	18.70171
63.344	18.70171
63.344	18.70171
63.336	18.71314
63.456	18.72457
63.44	18.70743
63.512	18.69029
63.576	18.672
63.64	18.65371
63.624	18.67771
63.76	18.70171

63.768	18.672
63.856	18.64229
63.96	18.648
63.928	18.65371
63.888	18.66629
63.968	18.67886
64.136	18.65486
64.088	18.63086
64.16	18.62514
64.2	18.61943
64.216	18.63086
64.208	18.64229
64.296	18.63086
64.376	18.61943
64.424	18.608
64.408	18.59657
64.472	18.61943
64.488	18.64229
64.552	18.61371
64.552	18.58514
64.6	18.57257
64.68	18.56
64.688	18.58971
64.8	18.61943
64.944	18.59543
64.904	18.57143
64.984	18.55429
64.968	18.53714
64.952	18.56686
65.056	18.59657
65.128	18.56114
65.136	18.52571
65.208	18.52
65.144	18.51429
65.128	18.52
65.192	18.52571
65.28	18.52571
65.424	18.52571
65.424	18.51429
65.4	18.50286
65.416	18.52571
65.496	18.54857
65.608	18.52571
65.6	18.50286
65.576	18.49714
65.624	18.49143

65.64	18.51429
65.672	18.53714
65.688	18.51429
65.784	18.49143
65.808	18.47886
65.864	18.46629
65.832	18.49029
65.864	18.51429
66.008	18.48457
66.04	18.45486
66.104	18.45486
66	18.45486
66.064	18.47314
66.064	18.49143
66.168	18.47886
66.288	18.46629
66.24	18.46057
66.176	18.45486
66.136	18.47314
66.24	18.49143
66.32	18.46743
66.296	18.44343
66.296	18.44343
66.312	18.44343
66.368	18.46057
66.352	18.47771
66.464	18.44914
66.456	18.42057
66.52	18.41486
66.488	18.40914
66.544	18.432
66.52	18.45486
66.616	18.43771
66.656	18.42057
66.696	18.41486
66.672	18.40914
66.728	18.42629
66.728	18.44343
66.824	18.432
66.864	18.42057
66.936	18.40343
66.848	18.38629
66.84	18.40914
66.792	18.432
66.96	18.40229
66.992	18.37257

67.032	18.37257
66.984	18.37257
67.016	18.40229
67.056	18.432
67.096	18.39657
67.2	18.36114
67.184	18.36114
67.184	18.36114
67.12	18.37943
67.152	18.39771
67.28	18.392
67.288	18.38629
67.312	18.37371
67.312	18.36114
67.296	18.37371
67.368	18.38629
67.4	18.36229
67.44	18.33829
67.472	18.33257
67.432	18.32686
67.488	18.35657
67.456	18.38629
67.544	18.35657
67.624	18.32686
67.616	18.32686
67.656	18.32686
67.6	18.34971
67.64	18.37257
67.744	18.34971
67.784	18.32686
67.824	18.32114
67.816	18.31543
67.816	18.32686
67.84	18.33829
67.92	18.33257
67.952	18.32686
67.992	18.32114
67.976	18.31543
67.92	18.33257
67.888	18.34971
68.008	18.33257
68.128	18.31543
68.064	18.304
68.048	18.29257
68	18.304
68.104	18.31543

68.144	18.304
68.192	18.29257
68.184	18.28
68.264	18.26743
68.208	18.30286
68.184	18.33829
68.288	18.30857
68.256	18.27886
68.368	18.27886
68.392	18.27886
68.36	18.29714
68.344	18.31543
68.424	18.29714
68.528	18.27886
68.48	18.27314
68.432	18.26743
68.488	18.28
68.536	18.29257
68.584	18.27429
68.656	18.256
68.6	18.26171
68.656	18.26743
68.512	18.28
68.664	18.29257
68.656	18.27429
68.704	18.256
68.728	18.24457
68.68	18.23314
68.712	18.256
68.76	18.27886
68.816	18.26743
68.832	18.256
68.848	18.24457
68.872	18.23314
68.824	18.256
68.888	18.27886
68.944	18.25029
68.96	18.22171
68.992	18.22171
69.072	18.22171
69.096	18.23314
69.136	18.24457
69.104	18.22171
69.168	18.19886
69.096	18.192
69.136	18.18514

69.096	18.20914
69.064	18.23314
69.208	18.20343
69.248	18.17371
69.136	18.17371
69.192	18.17371
69.104	18.18629
69.2	18.19886
69.296	18.18629
69.312	18.17371
69.312	18.17371
69.288	18.17371
69.192	18.19771
69.256	18.22171
69.272	18.19771
69.416	18.17371
69.36	18.168
69.312	18.16229
69.256	18.18629
69.4	18.21029
69.416	18.192
69.472	18.17371
69.544	18.16229
69.52	18.15086
69.512	18.18057
69.504	18.21029
69.56	18.18057
69.608	18.15086
69.584	18.14514
69.56	18.13943
69.512	18.15086
69.52	18.16229
69.536	18.15657
69.592	18.15086
69.592	18.13943
69.608	18.128
69.568	18.15086
69.608	18.17371
69.688	18.15657
69.664	18.13943
69.72	18.128
69.696	18.11657
69.616	18.13943
69.68	18.16229
69.632	18.14514
69.672	18.128

69.696	18.11657
69.64	18.10514
69.632	18.13371
69.656	18.16229
69.72	18.13943
69.768	18.11657
69.776	18.11657
69.632	18.11657
69.136	18.12
68.704	18.47

Appendix B

Single Panel Constant Solar Radiation Data:

110W/m^2	140W/m^2	180W/m^2	230W/m^2
10.378	15.837	21.824	23.517
9.959	15.418	20.929	22.533
9.809	15.247	20.219	21.803

Two Panels Constant Solar Radiation Data:

110 W/m^2	**140** W/m^2	**180** W/m^2	**230** W/m^2
10.645	19.159	29.934	40.711
10.054	17.888	28.08	38.535
9.939	16.826	27.377	37.597